Palaeobiodiversity and Palaeoenvironments
https://doi.org/10.1007/s12549-024-00608-3

SENCKENBERG

ORIGINAL PAPER

# Devonian to Mississippian strata of the Shine Jinst region revisited: Facies development and stratigraphy in southern Mongolia (Gobi Altai Terrane)

Peter Königshof[1] · Sarah K. Carmichael[2] · Johnny A. Waters[2] · Will Waters[3] · Ariuntogos Munkhjargal[1,4] · Sersmaa Gonchigdorj[4] · Catherine Crônier[5] · Atike Nazik[6] · Katie Duckett[2,7] · Jenny Foronda[2] · Johannes Zieger[8] · Ulf Linnemann[8]

Received: 15 January 2024 / Revised: 18 March 2024 / Accepted: 25 March 2024


## Abstract

This report provides new stratigraphical and facies data from Devonian and Carboniferous rocks in the Shine Jinst region (Trans Altai Zone, southern Mongolia) with a special focus on the Lower Devonian Chuluun Formation, the Middle Devonian Tsagaankhalga Formation, and the Upper Devonian to Mississippian Heermorit Member of the Indert Formation. Facies development in the Shine Jinst region exhibits a fundamental break in the carbonate platform evolution in the Lower Devonian as reef building organisms were affected by a major regression and deposition of several metres-thick conglomerates at the base of the Tsakhir Formation (Lower Devonian). The overlying Hurenboom Member of the Chuluun Formation is composed of fossiliferous limestones. Reef building organisms, such as colonial corals and stromatoporoids show low diversity and exhibit limited vertical growth and lateral extension of individuals. Thus, they do not represent a real reef as proposed in previous publications but biostromal limestones instead. One reason might be the isolated position of the Shine Jinst region between an unknown continent and a volcanic arc in the early Middle Devonian that hampered the successful colonization in shallow-water areas. Bivalves of the Alatoconchid family were once grouped into reef builders or biostrome builders and they are known only from Permian rocks. The found bivalve biostomes in Mongolia may represent precursors, which would document the oldest record of Alatoconchids found in the world. Remarkable thicknesses of massive crinoidal grainstones ("encrinites") are documented in many parts of the succession, which suggest rather stable environmental conditions of a carbonate ramp setting at different times. The occurrence of thick-bedded conglomerates in the Shine Jinst section is not restricted to the Lochkovian to Pragian interval (Tsakhir Formation), but also occurs in the Eifelian. A thick-bedded conglomerate, which is interpreted to represent braided fluvial or fan-delta to shallow-marine deposits occurs at the base of the Tsagaankhaalga Formation. A steep relief associated with uplift and volcanism seems to be a realistic scenario for deposition of these sediments. This succession points to a remarkable tectonic uplift or sea-level fall in the Middle Devonian. Conodont findings of the studied section confirm the occurrence of time-equivalent strata of the Choteč Event, the Dasberg Crisis, and the Hangenberg Event found elsewhere in the world, which are described from Mongolia for the first time. Sedimentological descriptions, revised biostratigraphical data, and U-Pb dating by LA ICP-MS of some volcaniclastic rocks from the Chuluun Formation are presented in this report. The studied section records a complex interaction of sedimentation, regional tectonics, sea-level changes and coeval volcanism, which is very similar to other regions in Mongolia. The new data provide the background for further scientific studies in this region. This is a contribution to the Special Series on "The Central Asian Orogenic Belt (CAOB) during Late Devonian: New insights from southern Mongolia", published in this journal.

**Keywords** Central Asian Orogenic Belt · Biostratigraphy · Mongolian Terranes · Devonian Events · Zircon Geochronology

## Introduction

Southern Mongolia is centrally located within the Central Asian Orogenic Belt (CAOB), which is the world`s largest Palaeozoic accretionary orogenic belt (Şengör et al. 1993).

This is a contribution to a special series on "The Central Asian Orogenic Belt (CAOB) during Late Devonian: new insights from southern Mongolia."

Extended author information available on the last page of the article

Published online: 31 May 2024

The CAOB is subdivided in two structural units, a Neoproterozoic northern unit and an early Palaeozoic southern unit, which are separated by the Main Mongolian Lineament (Tomurtogoo 1997). These units were subdivided into different zones (terranes) and blocks. The accretionary system has been evolved from the Neoproterozoic time until the Cenozoic (Safanova et al. 2017) and includes oceanic, intra-oceanic, and numerous fragments of Precambrian microcontinents and collisional and post-collisional complexes as well as continental margin arc terranes. Significant progress has been made in understanding the complex plate tectonic dynamics by studies on geochronological, geochemical, and isotope dating preferably from magmatic and metamorphic rocks (Badarch et al. 2002; Windley et al. 2007; Macdonald et al. 2009; Lehmann et al. 2010; Xiao et al. 2010; Kröner et al. 2010, 2014; Gibson et al. 2013; Xiao and Santosh 2014; Safonova et al. 2017; Yang et al. 2019). The CAOB was formed by the suturing of the Palaeo-Asian Ocean (PAO) and multi-stage Palaeozoic collisions of the East European -, Siberian -, North China -, and Tarim cratons. The subduction of the PAO continued during the middle and late Palaeozoic before final closure of this ocean and its Turkestan and Junggar branches during the late Palaeozoic to the Mesozoic (Windley et al. 2007; Xiao et al. 2008; Donskaya et al. 2013; Yang et al. 2015; Safonova et al. 2017). Although several petrological, geochemical, and structural studies were conducted to get a better understanding of the complex CAOB framework, detailed sedimentological/facies and stratigraphical descriptions are rare (e.g. Over et al. 2011; Pellegrini et al. 2012; Gibson et al. 2013; Sullivan et al. 2016; Cronier et al. 2021; Munkhjargal et al. 2021a, b; Nazik et al. 2021; Roelofs et al. 2021; Waters et al. 2021). Those studies are necessary in order to reconstruct the complex depositional and tectonic history of the region, and to decipher regional relationships with adjacent tectonic blocks. A general stratigraphical background and facies description of the Shine Jinst region was provided in the frame of the Mongolian-Russian expeditions in the 1970`s and later as a result of the International Geoscience Programms (IGCP`s 410 and 421), and sporadic reports provided information on different fossil groups and stratigraphy of this region (e.g. Ulitina et al. 1976; Rozman and Minjin 1988; Alekseeva et al. 1996; Minjin et al. 2001; Wang et al. 2003, 2005a, b; Over et al. 2011; Sullivan et al. 2016). Conodont stratigraphy for instance has been improved since the last decades and new conodont zones are applied (e.g. Becker et al. 2016), thus revision of earlier collections and new samples are necessary to constrain the depositional history/stratigraphy of this relatively unexplored region. In this paper, we present an overview of Devonian rocks in the Shine Jinst region as a result of an expedition in 2022 with a special focus on the biostratigraphic frame of the Lower Devonian Chuluun Formation, the Middle Devonian Tsagaankhaalga Formation, and the Upper Devonian to Mississippian Heermorit Member of the Indert Formation.

## Geological setting, study location and stratigraphic overview

The Shine Jinst region is located in the Gobi-Altai Zone of southern Mongolia (Fig. 1). According to Kröner et al. (2010), its southern margin is defined by the Trans-Altai Fault, which is in contact with the Palaeozoic oceanic domain of the Trans-Altai Zone. The region south of the Trans-Altai Fault was divided into a variety of zones and terranes by various authors (e.g. Ruzhentsev and Pospelov 1992; Badarch et al. 2002). Herein, we follow the subdivision by Kröner et al. (2010) who proposed a revised geodynamic model for the evolution of SW Mongolia in the Palaeozoic. According to this study, the Trans-Altai Zone was subdivided from north to south into the Khuvinkharin Subzone, the Edrengin Subzone, and the Dzolen Subzone. Further to the south the South Gobi Zone occurs. The latter one was an active accretionary arc system until the end of the Palaeozoic (Lamb and Bardach 1997) when the PAO culminated in the collision of the northern China and southern Mongolia (e.g. Xiao et al. 2008, 2010; Chen et al. 2010). Based on detrital zircon studies from Ordovician to Lower Devonian rocks the area was formed as an oceanic basin trapped between an unidentified continent and an offshore island-arc complex (Lamb et al. 2008; Gibson 2010), which is supported by the large thickness of volcanic rocks in the entire succession. The complex depositional history was later affected by post-Palaeozoic tectonic implications. Lamb et al. (2008) have shown that the tectonic and sedimentary setting changed from a convergent margin to an intracontinental setting with sinistral transpression. Later, in the Jurassic a left-lateral strike-slip system developed in Asia, which included two major faults, the Tost Fault and the Gobi Onon Fault in southern Mongolia (Fig. 1a). According to Lamb et al. (2008) these faults have the same orientation and sense of motion as left-lateral faults and associated wrench thrust faults in the Shine Jinst region. Intracontinental deformation also occurred during the Cenozoic (Lamb et al. 2008; Cunningham 2010), resulting in a complex tectonic framework of the entire Shine Jinst region (Fig. 1b–d). Palaeogeographically, this region was located approximately 35° N of the equator (Copper and Scotese 2003) and average sea surface temperatures are estimated to have been around 30°C in the Early Devonian (Copper 2002).

The oldest strata exposed in the south-eastern part of the Shine Jinst region consist of Lower Ordovician rocks of the Daravgai Formation, which are conformably overlain by the Gashuun-Ovoo Formation. The thicknesses of Ordovician rocks vary from 1300 m to 2000 m and sediments are mainly composed of carbonates, whereas sandstones are less frequent (Minjin et al. 2001). Ordovician and Silurian successions are dominated by limestones. Reefs grew and produced a rimmed shelf during the lower Silurian until tectonic

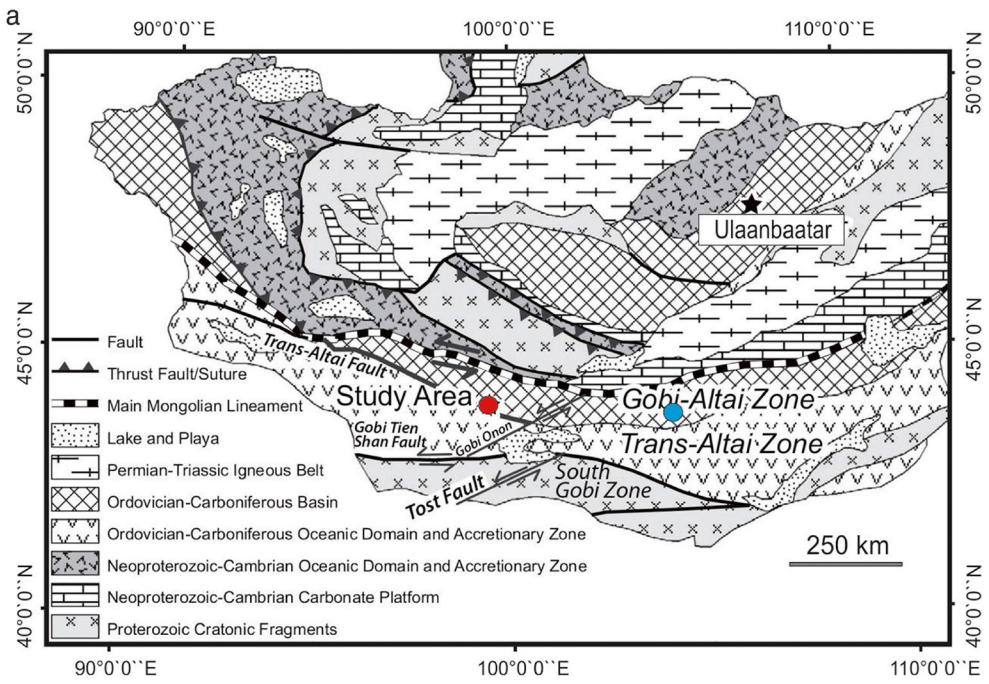


**Fig. 1** **a** Tectonic map of Mongolia (reused from Gibson et al. 2013) based on modifications from Macdonald et al. (2009), and Kröner et al. (2010). *Red circle* study area, *blue circle* studied section within the Mandalovoo Subzone (defined as Mandalovoo Terrane by Badarch et al. 2002) based on data by Munkhjargal et al. (2021)

induced regression and siliciclastic sedimentation terminated carbonate platform sedimentation in the late Silurian–Early Devonian (Soja et al. 2010; Gibson et al. 2013). Silurian and Lower Devonian rocks are subdivided into the Shachuluut-, the Tsagaanbulag-, and the Amansair Formation (Fig. 2), which are composed of limestones, siltstones and sandstones. The Tsagaanbulag Formation rests upon the Silurian Shachuluut Formation, a hiatus cannot be excluded. The upper part of the Tsagaanbulag Formation is assigned to middle Lochkovian, whereas the stratigraphy of the lower part is still unclear (Wang et al. 2005a). Thus, the Silurian/Devonian boundary is not clearly defined. Chemostratigraphy was used to get better results (Reitman 2010), and the author concluded that the Silurian-Devonian boundary may be higher in the Tsagaanbulag Formation based on $\delta^{13}$ C isotope data but further sampling is necessary to determine the precise boundary.

The overlying Amansair Formation has a stratigraphical range from the upper Lochkovian to Pragian. This formation is unconformably overlain by the Lower Devonian Tsakhir Formation representing a sharp contact due to uplift and erosion of older rocks (Lamb and Badarch 1997). Due to erosion, the Tsakhir Formation overlies different horizons of the underlying Amansair Formation. The thickness of the Tsakhir Formation varies between 540–720 m (Minjin et al. 2001). The base of the Tsakhir Formation consists of massive cobble conglomerates, which are dominated by limestone clasts that were sourced by underlying, mainly Silurian units. The succession fines upward to interbedded conglomerates and sandstones, interbedded sandstones, grainstones, siltstones and mudstones (Gibson et al. 2013). Felsic volcanic deposits also exist in the upper part of this succession. The formation was interpreted to represent braided fluvial or fan-delta to shallow-marine deposits (Lamb and Badarch 1997, 2001). The Tsakhir Formation is conformably overlain by the Lower Devonian (?Emsian to Eifelian) Chuluun Formation. The Chuluun Formation marks the beginning of detailed sampling of our section, although we took some spot samples for biostratigraphic studies in the Shine Jinst region from older successions as well. The Chuluun Formation was subdivided into two members, the Hurenboom Member and the Volcanic Carbonate Member (Alekseeva 1993). The Chuluun Formation is disconformably overlain by the Tsagaankhaalga Formation, which starts with a conglomerate and has a total thickness of about 200 m. Wang et al. (2005b) and Over et al. (2011) assigned this formation to the early Eifelian according to their described conodont fauna. This formation is conformably overlain by poorly fossiliferous, mainly volcaniclastic deposits of the Gobi-Altai Formation. The Gobi-Altai Formation is composed of the lower Tentaculite Member and the upper Khar Member and was assigned to Givetian to early Famennian by Minjin et al. (2001). Biostratigraphic results by Sullivan et al. (2016) suggest an early to middle Givetian age, but the detailed stratigraphic range of the Gobi-Altai Formation remains

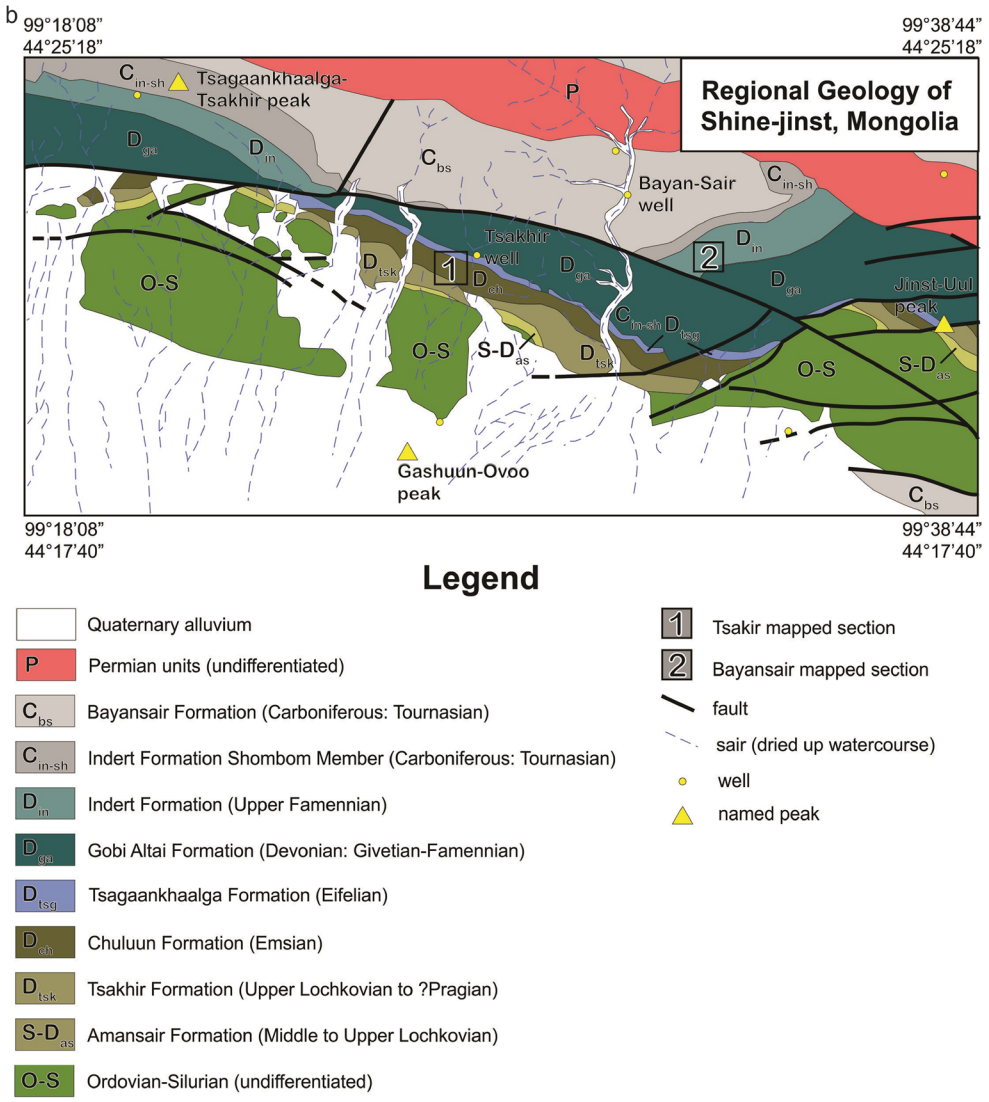


**Fig. 1 b** Geological map of the study area according to Wang et al. (2005a). Numbers 1 and 2 show the position of the sections (compare detailed maps of figures 1c and 1d)

uncertain. The youngest formation of the section is represented by the Indert Formation, which is subdivided into the Heermorit Member and the Shombon Member (Fig. 2). The age of the Heermorit Member is still questionable, as it was first correlated with Famennian (Minjin et al. 2001) and later it was considered as latest Famennian and early Carboniferous (Wang et al. 2005a). The Shombon Member was assigned to early Carboniferous (Tournaisian) by Minjin et al. (2001).

## Material and methods

This research is based on field observations, polished and etched slabs, and biostratigraphy of most important successions of the section. The section was measured bed by bed at cm scale, and 298 rock samples were taken for geochemical analysis, sedimentology, and biostratigraphy. Polished slabs and hand-samples are stored at the Senckenberg Research Institute and Natural History Museum Frankfurt, Germany, under repository numbers SMF 99299 to SMF 99349. Additionally, 101 carbonate samples were dissolved for conodont biostratigraphy according the preparation method described in Ta et al. (2022). Whole rock samples of 1.5 to 3.2 kg each were dissolved. Out of 101 samples 47 were productive so far (work in progress, some samples require further liquid separation and picking). The overall number of conodont specimens is rare, which is comparable to a sampled section in southern Mongolia (Wang et al. 2005a, b; Munkhjargal et al. 2021b) and previous conodont studies of this region (e.g. Wang et al. 2005a, b; Sullivan et al. 2016). Several conodont specimens of biostratigraphic significance were mounted on slides and

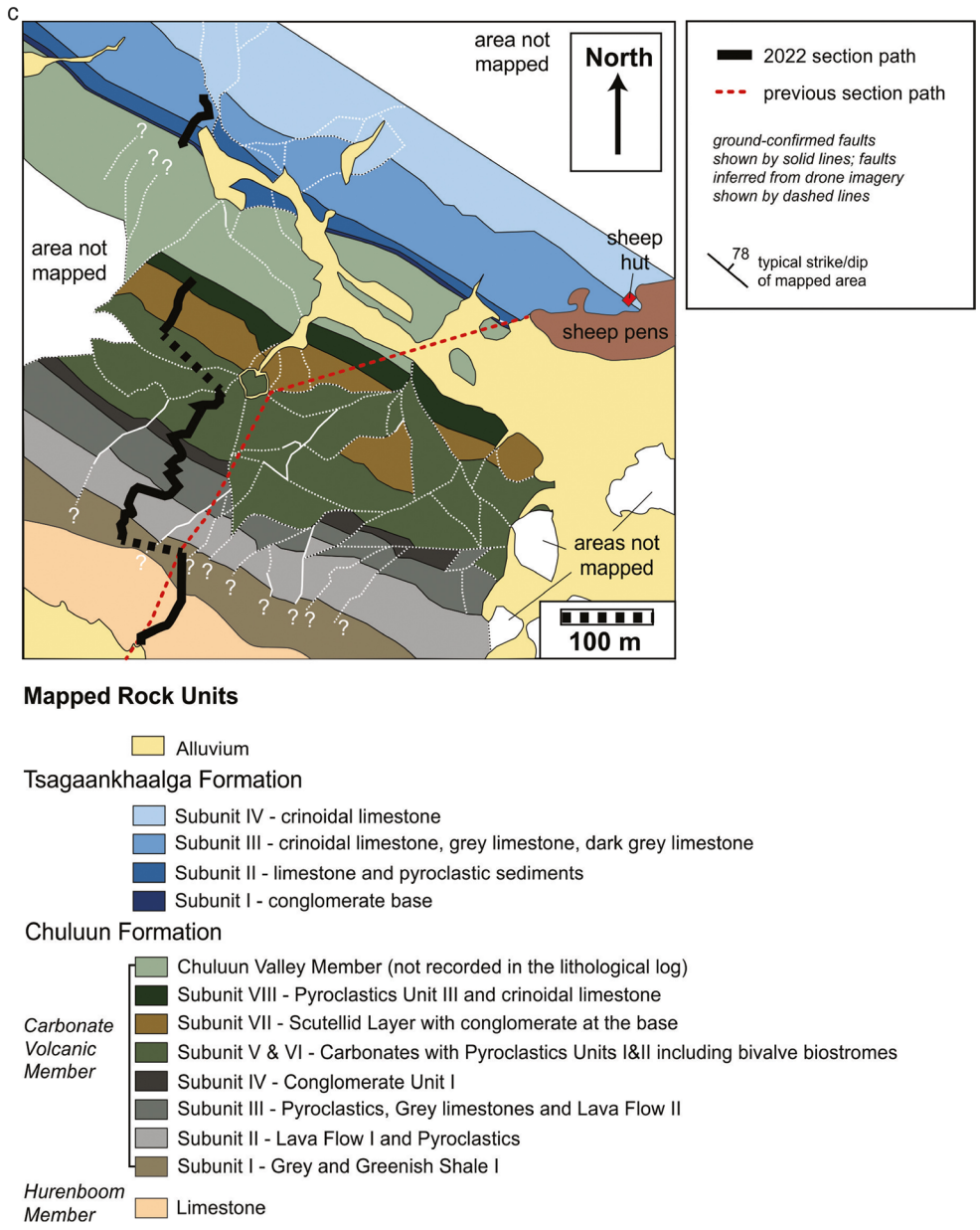


**Fig. 1 c** Detailed geological map provided by the field trip in 2022 of the Tsakir well area (#1 in figure 1b). Note that the inofficial Chuluun Valley Member is not included in the lithological log (Figs. 8a-c)

sputtered with a Gold-Platinium alloy, and imaged on a scanning electron microscope. The material described and figured herein is stored at the Mongolian University of Sciences and Technology, Ulaanbaatar, Mongolia.

As the entire succession contains a number of volcanic ash layers we took some samples for U-Pb dating. Zircon concentrates were separated from 1 to 2kg whole rock material at the Senckenberg Naturhistorische Sammlungen Dresden (Museum für Mineralogie und Geologie, Sektion Geochronologie, GeoPlasmaLab). After crushing up of the fresh sample in a jaw crusher, material was sieved for the fraction from 36 to 400 µm. Heavy mineral separation was achieved from this fraction using LST (lithium heteropolytungstate in water) prior to magnetic separation in the Frantz isomagnetic separator. Final selection of the zircon grains for U-Pb dating was achieved by hand-picking under a binocular microscope. When possible, at least 150 zircon grains of all grain sizes and morphological types were selected (Fedo et al. 2003; Link et al. 2005), mounted in resin blocks, and polished to half their thickness. Cathodoluminescence (CL)-imaging was performed using a ZEISS SEM EVO 50 coupled to a HONOLD CL detector operating with a spot

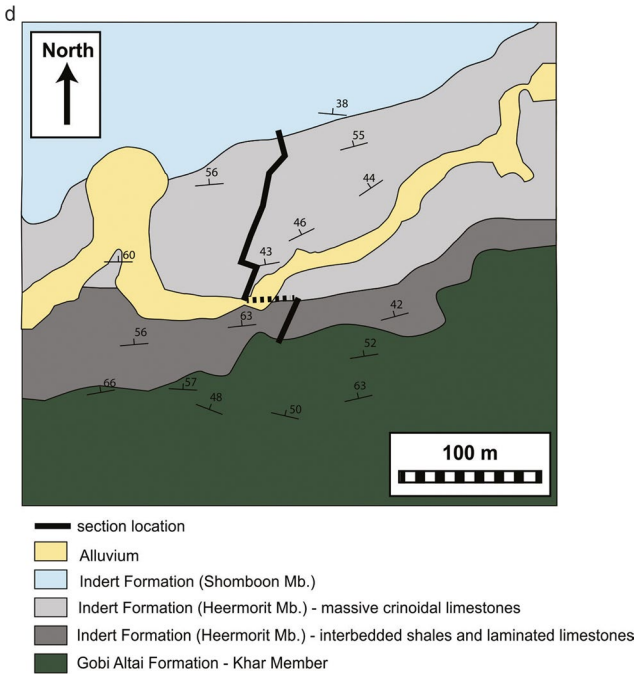


**Fig. 1 d** Detailed geological map provided by the field trip in 2022 of the Bayansair area (#2 in Fig 1b)

size of 550 nm at 20 kV. Zircons were analysed for U, Th, and Pb isotopes by LA-ICP-MS techniques at the Museum für Mineralogie und Geologie (GeoPlasma Lab, Senckenberg Naturhistorische Sammlungen Dresden), using a Thermo Fisher Scientific Element XR sector field ICP-MS (single-collector) coupled to a RESOlution 193 nm excimer laser. Each analysis consisted of approximately 15 s background acquisition followed by 30 s data acquisition, using a laser spot size of 25 and 35 µm, respectively. A common Pb correction based on the interference- and background-corrected $^{204}$Pb signal and a model Pb composition (Stacey and Kramers 1975) was carried out if necessary. The necessity of the correction is judged on whether the corrected $^{207}$Pb/$^{206}$Pb lies outside of the internal errors of the measured ratios (Frei and Gerdes 2009). Discordant analyses were generally interpreted with care. Raw data were corrected for background signal, common Pb, laser-induced elemental fractionation, instrumental mass discrimination, and time-dependant elemental fractionation of Pb/Th and Pb/U using a Microsoft Excel ® spreadsheet developed by Richard Albert Roper and Axel Gerdes (FIERCE, Institute of Geosciences, Johann Wolfgang Goethe-University Frankfurt, Frankfurt am Main, Germany). Reported uncertainties were propagated by quadratic addition of the external reproducibility obtained from the reference zircon GJ-1 (~0.6% and 0.5-1% for the $^{207}$Pb/$^{206}$Pb and $^{206}$Pb/$^{238}$U, respectively; Jackson et al. 2004) during individual analytical sessions and within-run precision of each analysis. In order to test the accuracy of the measurements and data reduction, we included the Plešovice zircon as a secondary reference in our analyses and which gave reproducibly ages of 337 Ma, fitting with the results of Sláma et al. (2008). As an additional secondary reference, the Temora zircon (417 Ma, Black et al. (2003) were included into the analytical procedure. Concordia ages (95% confidence level) were produced using Isoplot/Ex 4.15 (Ludwig 2008). The $^{207}$Pb-$^{206}$Pb age was taken for interpretation for all zircons > 1.5 Ga (Puetz 2018), and the $^{206}$Pb-$^{238}$U ages for younger grains. For further details on analytical protocol and data processing see Gerdes and Zeh (2006). Zircon grains showing a degree of concordance in the range of 90-110% in this paper were used for interpretation. U and Pb content and Th/U ratio were calculated relative to the GJ-1 zircon reference and are accurate to approximately 10%. Analytical results of U-Th-Pb isotopes and calculated U-Pb ages are given in Tables 1 and 2 (electronical supplement).

## Results

### Biostratigraphy

Herein we present new biostratigraphic data based on conodonts of most important successions, which resulted from our field trip in 2022. Stratigraphically important fossils from earlier publications are included in this report. Due to the large number of conodont samples and very voluminous residues, this work is not completely finished. Numerous conodont samples were barren (approximately 50%) and productive samples yielded 1 – 5 specimens per kg on average. Most diagnostic taxa beside others figured herein are from already studied parts of the succession, in order to get better stratigraphic ranges of the formations or members. Due to our study, we could fundamentally improve the conodont record and we also could pinpoint three Devonian events in Mongolia for the first time, the Choteč Event, the Dasberg Crisis, and the Hangenberg Event.

Generally, conodont specimens are moderately preserved, many were fragmented and partially recrystallized. Carboniferous specimens are well preserved. The Conodont Color Alteration Index (CAI) ranges between CAI 4.5 for delicate and/or juvenile forms, and CAI 5 to CAI 5.5 for adult forms. Biostratigraphy based on conodonts is difficult in southern Mongolia as the overall conodont abundance is rather low in comparison to coeval pelagic successions elsewhere. Although conodont data were published by Alekseeva et al. (1996), Minjin et al. (2001) and later by Wang et al. (2003, 2005a, b) most zonal index species have not been found, or other important findings were not illustrated (Nyamsuren 1999) and, thus, determinations remain dubious.

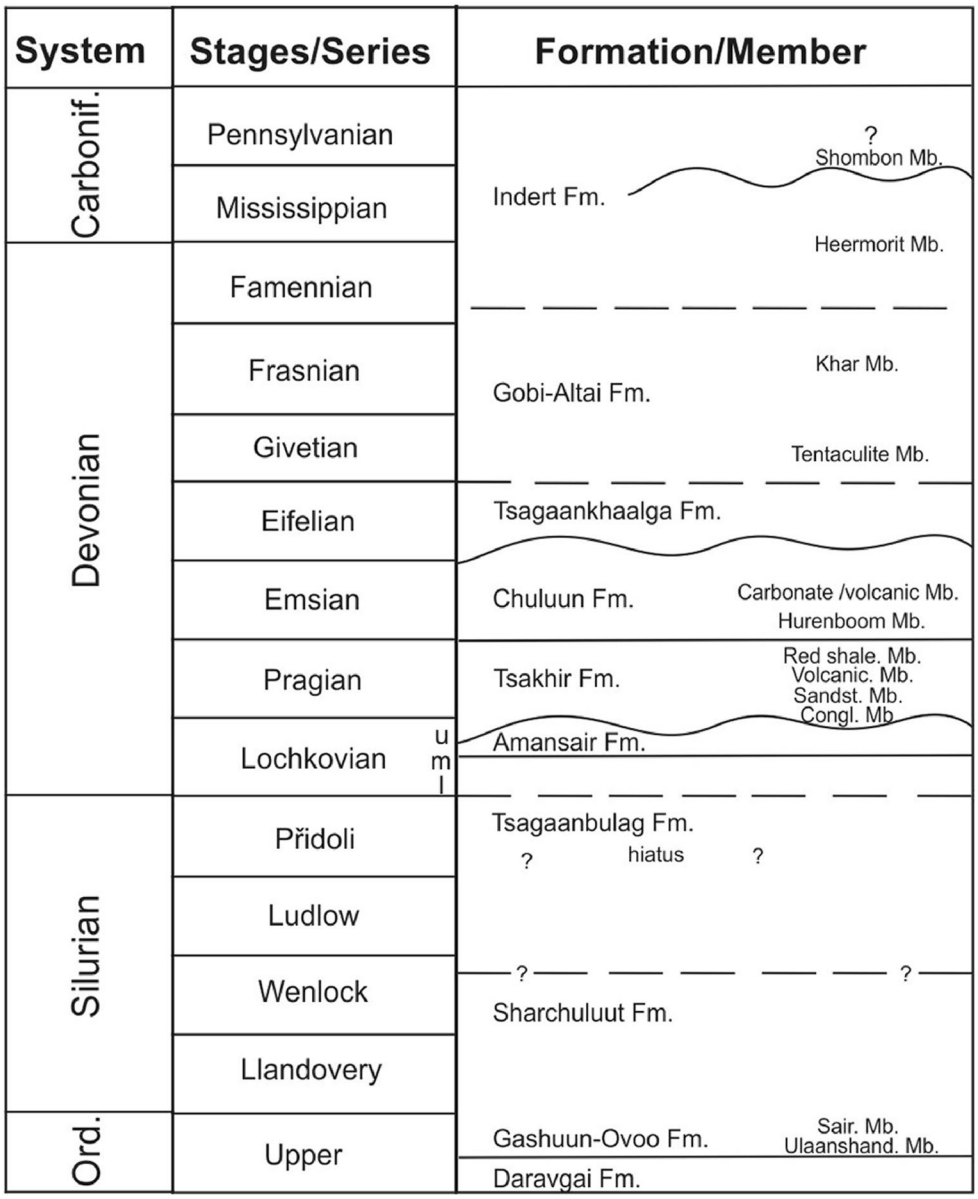


**Fig. 2:** Stratigraphy of the Shine Jinst region of southern Mongolia. Compiled after Rozman and Minjin (1988), Alekseeva (1993), Wang et al. (2005a), and Gibson et al. (2013) and own data. The wavy lines represent erosional unconformities. The stippled line across the Silurian/Devonian rocks are related to lateral facies differences. The stippled line between the Eifelian and Givetian stages point to uncertain stratigraphical ranges of the Tsagaankhaalga- and the Gobi-Altai formations

Conodonts from the Amansair Formation

The Amansair Formation has a thickness of 250–295 m and ranges from late Silurian to Early Devonian (Minjin et al. 2001; Lamb et al. 2008). Conodont record is scarce, findings of the conodont species *Lanea omoalpha* suggest a lower to middle Lochkovian age (Murphy and Valenzuela-Rios 1999; Corriga et al. 2016; Corriga and Corradini 2009). This species has its first appearance in the *Icriodus postwoschmidti* Zone (Corradini and Corriga 2012) as reported from the Carnic Alps (Corriga et al. 2016). Macrofossils (corals, brachiopods) point to a stratigraphical range from Přidoli to Lochkovian. We have found a spathognathodontid specimen, which may belong to the genera *Zieglerodina*? sp. in sample SH-C-4 (N 44° 21`35,1``, E 99° 26`44,9``, see Fig. 3) in a bioclastic wackestone of the Amansair Formation, which disconformably underlies the Tsakhir Formation. Furthermore, a questionable *Pandorinellina* sp. (could be *Pandorinellina praeoptima*) was found in the same sample. Limestones of the Amansair Formation are not completely dissolved yet, so we expect to get much better biostratigraphic results in future. Nevertheless, the found specimens point to a Lochkovian to Pragian age.

Conodonts from the Chuluun Formation

We began detailed sampling from the Chuluun Formation and have found *Bellodella resima* (Fig. 3) in sample SH-C-16 (Hurenboom Member, see Fig. 4a) and some broken, undeterminable conodonts. Higher in the section (sample

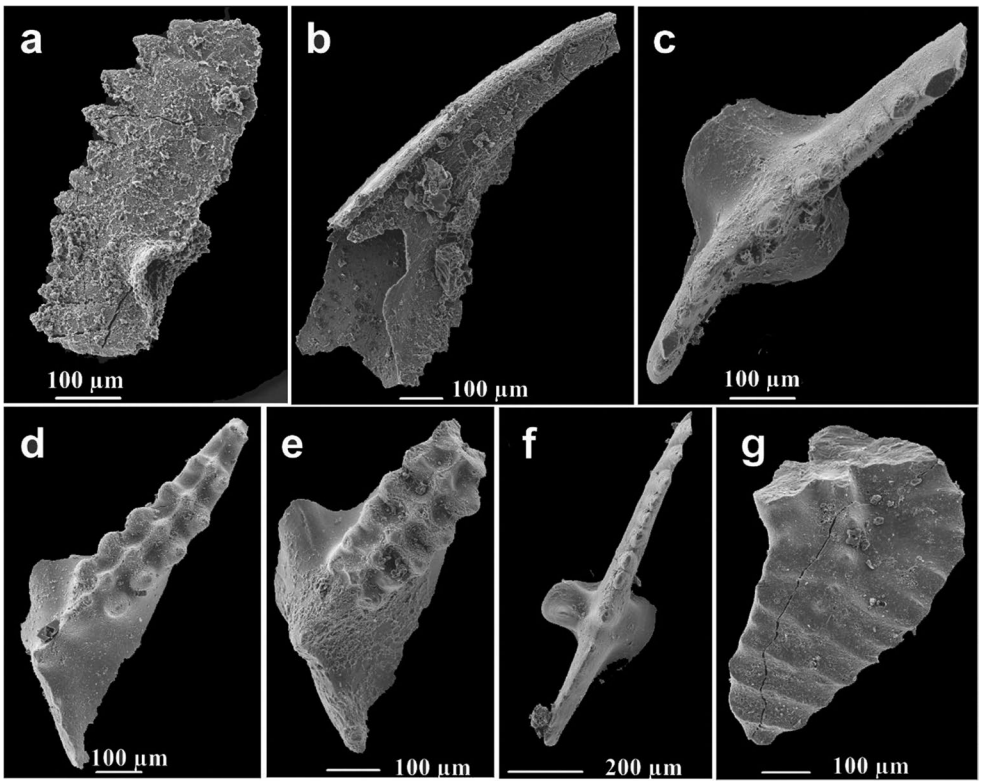


**Fig. 3:** Conodonts from the Amansair Formation and the Chuluun Formation. **a** *Zieglerodina*? sp. (sample SH-C-4, Amansair Formation); **b** *Bellodella resima* Philip, 1965 (sample SH-C-16, Chuluun Formation); **c** *Criteriognathus steinhornensis* Ziegler, 1956 (sample SH-C-20); **d** *Latericriodus bilatericrescens bilatericrescens* Ziegler, 1956 (sample SH-C-20, Chuluun Formation); **e** *Latericriodus bilatericrescens bilatericrescens* Ziegler, 1956 (broken specimen, sample SH-C-32); **f** *Criteriognathus steinhornensis* Ziegler, 1956 (sample SH-C-32); **g** *Eolinguipolygnathus* cf. *catharinae* Bultynck, 1989 (sample SH-C-32, broken specimen)

SH-C-20) we have found rare *Latericriodus bilatericrescens bilatericrescens* and *Criteriognathus* cf. *steinhornensis*, which were described by Carls and Gandl (1969) from lower Emsian rocks. According to Aboussalam et al. (2015), this subspecies ranges from the Lower *bilatericrescens* Zone (icriodontid zonation) to the basal upper Emsian *fusiformis* Zone. Aboussalam et al. (2015) have shown that the *bilatericrescens* Zone correlates with the higher part of the *excavatus* morphotype 114 Zone (global polygnathid Zonation). Together with *Criteriognathus* cf. *steinhornensis* (name-giving ozarkonidid Zonation), which occurs in the same sample a late early Emsian age of sample SH-C-20) is confirmed. Higher in the section, sample SH-C-32 yielded *Latericriodus bilatericrescens bilatericrescens* and *Criteriognathus steinhornensis* and a questionable (incomplete) *Eolinguipolygnathus* cf. *catharinae*. (Fig. 3). The latter one is the name-giving species for the *catharinae* Subzone, which is younger then conodonts found in sample SH-C-30. Conodonts *Polygnathus pugiunculus* and *Polygnathus snigirevae* are reported from the Chluluun Formation by Wang et al. (2003) point to upper Emsian, which were found in higher parts of their record.

Conodonts from the Tsagaankhaalga Formation

According to Wang et al. (2005a, b) and Chuluun et al. (2005) the Tsagaankhaalga Formation is Eifelian in age. Our data support these results (Fig. 4). We have found some conodonts specimens from the black limestone and shale interval (see Figs. 8c and 11). The conodont diversity is low as well as the number of specimens, which yield icriodontids only. We found *Caudicriodus angustus cauda*, *Caudicriodus declinatus*, *Caudicriodus strelcki*, *Caudicriodus angustus angustus* (sample SH-C-46 to sample SH-C-48), *Icriodus regularicrescens* and *Icriodus* cf. *corniger corniger* (Fig. 4). *Icriodus corniger corniger* was restricted to the *partitus* and *costatus* Zones (Weddige 1977), whereas Bultynck (1985) reported the same species ranging from the *serotinus* Zone to the *costatus* Zone. *Icriodus corniger corniger* was found in sample SH-C-43 (Fig. 8c). *Caudicriodus declinatus* and *Caudicriodus angustus cauda* seem to be endemic, whereas *Caudicriodus angustus angustus* and *Caudicriodus stelcki* were reported from the USA, Canada, and Asia (e.g. Stewart and Sweet 1956; Klapper and Ziegler 1967; Bardashev 1990; Klug, 1983; Uyeno 1991; Uyeno and Lesperance 1997) from the Eifelian stage (*Po. costatus* Zone to *T. kockelianus* Zone).

The occurrence of *I. regularicrescens* (sample SH-C-48), which enters in approximately of the middle of the Eifelian (*Polygnathus pseudofoliatus* Zone) represents the youngest part of the greyish limestone succession. Polygnathids do not occur and thus, it is not possible to present a more detailed stratigraphy. *Caudicriodus angustus angustus* and *Caudicriodus stelcki* have been interpreted to represent rather cooler water specimens (Stewart and Sweet 1956; Uyeno and Lesperance 1997). Based on the stratigraphic range of these

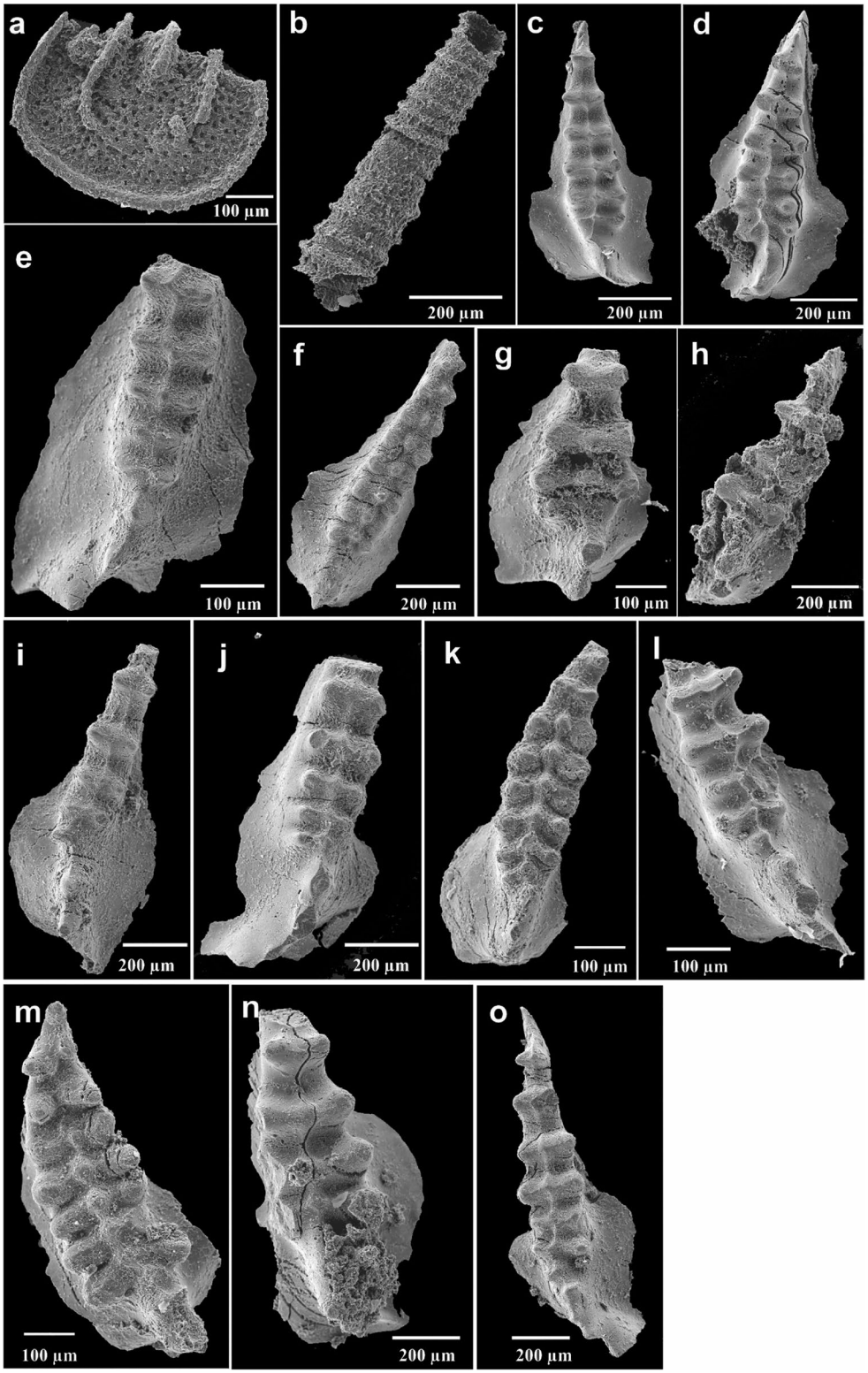


**Fig. 4:** Microfossils from the Tsagaankhaalga Formation. Ostracods and dacryoconarids will be published separately as determination is work in progress. **a** Endemic ostracod, Drepanellid sp. (sample SH-C-45, Tsagaankhaalga Formation); **b** Nowakia sp. (sample SH-C-43, Tsagaankhaalga Formation). Conodonts figured from "c" to "n" are sampled from the Tsagaankhaalga Formation. **c** *Caudicriodus angustus cauda* Wang and Weddige, 2005 in Wang et al. 2005b (sample SH-C-46); **d** *Caudicriodus declinatus* Wang and Weddige, 2005 in Wang et al. 2005b (sample SH-C-43); **e** *Caudicriodus* cf. *stelcki* Chatterton, 1974; incomplete specimen (sample SH-C-45); **f** *Icriodus regularicrescens* Bultynck, 1979 (sample SH-C-48); **g** *Caudicriodus stelcki* Chatterton, 1974 (sample SH-C-46); **h** *Caudicriodus* cf. *angustus angustus* Steward and Sweet, 1956 (sample SH-C-46); **i** *Caudicriodus angustus cauda* Wang and Weddige, 2005 in Wang et al. 2005b (sample SH-C-47). **j** *Caudicriodus angustus angustus* Steward and Sweet, 1956 (sample SH-C-47); **k** *Icriodus* cf. *corniger corniger* Wittekindt, 1966 (sample SH-C-43); **l** *Caudicriodus angustus angustus* Steward and Sweet, 1956 (sample SH-C-48); **m** *Caudicriodus declinatus* Wang and Weddige, 2005 in Wang et al. 2005b (sample SH-C-48); **n** *Caudicriodus* sp. (sample SH-C-48). **o** *Caudicriodus angustus cauda* Wang and Weddige, 2005 in Wang et al. 2005b (sample SH-C-48)

shallow-water succession the dark-grey limestones represent sediments of the Choteč Event. The short event interval falls into the top of the basal Eifelian *partitus* Zone and is marked by the maximum flooding of eustatic Depophase Ic2 (Becker et al. 2012). It is interesting to note that this event is also characterised by the spread of *Nowakia sulcata sulcata.* In our section large numbers of dacryoconarids occur in sample SH-C-44, SH-C-45, and SH-C-46 (Fig. 8c). So far, we have

not found diagnostic conodonts from the next younger Gobi Altai Formation but Sullivan et al. (2016) reported some diagnostic taxa from this formation, which suggest an age of Lower to Middle *varcus* Zone.

Conodonts from the Indert Formation

Carbonates at the base of the Indert Formation yielded some conodonts, which stratigraphically point to the Upper Famennian. The base of this part of the section contains thin-bedded black limestones and shales and might be incomplete due to small thrusts. Thus, we sampled a succession, which occurs approximately 100 m in the east (see Fig. 8d) which is a coeval succession, but more complete. Both sections yielded nearly the same conodont assemblage, which shows a stratigraphic range from the *Bispathodus aculeatus aculeatus* Zone to the *Bispathodus costatus* Zone (Spalletta et al. 2017; = Middle *expansa* Zone of Ziegler and Sandberg 1990). An important conodont is *Bispathodus aculeatus aculeatus*, which defines the lower boundary of the name-giving conodont zone was found in sample SHB-C-1. A questionable ?*Clydagnathus plumulus* was also found in the same sample. This species first appears at or near the base of the *Bispathodus aculeatus aculeatus* Zone. These conodonts are accompanied by *Pseudopolygnathus primus*, *Polygnathus communis communis,* and *Palmatolepis gracilis sigmoidalis,* and ramiform elements. *Polygnathus inornatus* has its first appearance in the *Bispathodus costatus* Zone (equivalent of the upper part of the Middle *expansa* Zone, Bahrami et al. 2011) and was found in sample SHB-C-3 (Fig. 5; Fig. 8d). Thus, the base of the Indert Formation (Heermorit Member), which is composed of dark-grey and black limestones is late Famennian (*Bispathodus aculeatus aculeatus* Zone to the *Bispathodus costatus* Zone) in age.

This succession covers the Dasberg Crisis (e.g. Hartenfels 2011, cum lit.), which is recognised for the first time from Mongolia. The next sample which yielded conodonts is sample SHB-C-16. *Bispathodus* cf. *costatus*, *Polygnathus vogesi*, *Bispathodus stabilis*, and *Pseudopolygnathus primus* were found (Fig. 6). Sample SHB-C-18 yielded similar conodont association plus *Polygnathus communis communis*. The lower part of column "b" of the Indert Formation (Heermorit Member, sample SH-B-C-33) yielded the following conodont assemblage: *Polygnathus communis communis*, *Polygnathus vogesi*, and *Polygnathus purus purus* among rare ramiform elements. According to Spalletta et al. (2017) *Polygnathus purus purus* appears in the *ultimus* Zone for the first time. The zonal index species *Bispathodus ultimus* was not found. Higher in the section, sample SHB-C-38 yielded *Bispathodus stabilis*, *Polygnathus communis communis*, a questionable *Protognathodus* cf. *meischneri*, and *Protognathodus kockeli* (Fig. 6). *Protognathodus kockeli* appears just after the Hangenberg Event and ranges to the *sandbergi* Zone (Lane et al. 1980). This species is the name-giving species of the revised conodont zones in the latest Famennian (Corradini et al. 2011; Spalletta et al. 2017) and is equivalent to the Upper *praesulcata* and *sulcata* zones of Ziegler and Sandberg (1984). The black shales below sample SHB-C-38 most probably are equivalents of the Hangenberg Black Shale (see Kaiser et al. 2016).

The next productive conodont sample is SHB-C-40 yielding *Polygnathus purus purus*, *Polygnathus* sp., *Polygnathus communis communis*, and *Siphonodella duplicata*, which is the index species of the lower Carboniferous *duplicata* Zone (Fig. 6). Many samples were barren while some others are still in progress and it might be that we can further improve the biostratigraphy in future. According to Minjin et al. (2001) the 360 m thick Shombon Member, which unconformably overlies the Heermorit Member is composed of white variously stratified, siliceous limestones. Brachiopods, crinoids, small corals, ostracods, gastropods, and Tournaisian conodonts of the *Scaliognathus anchoralis–Doliognathus latus* Zone have been found.

## Geochronology

In order to get additional stratigraphic data from the shallow-water Chuluun Formation we took four samples for zircon U-Pb dating. As the entire succession contains a large number of volcaniclastic deposits, we took the following samples from the Carbonate-Volcanic Member of the Chuluun Formation: samples SH-S-18 and SH-S-21 (both volcanic ashes), sample SH-S-32 (volcaniclastic rock), and sample SH-S-41 (greenish shale with large amount of volcanic ash). Samples exhibit the following results: samples getting younger from samples SH-S-18 at the base to sample SH-S-41 (404.9 ± 2.8 Ma to 400.1 ± 2.3 Ma) close to the top of the Carbonate-Volcanic Member. The overall magmatic age confirms a late Early Devonian (Emsian) age (Fig. 7) which is consistent with conodont data reported herein.

In samples SHB-G-23 and SHB-G-24b (both volcanic ashes) of the Indert Formation (Fig. 8) only inherited, very few old zircons were found and, thus, have been not useful for U-Pb dating.

## Lithofacies and facies development

The description starts from the base of the succession to the top in order to be consistent with the facies development during deposition. We measured different sections, focusing on the Chuluun Formation, the Tsagaankhaalga Formation, and the Indert Formation (Heermorit Member; Devonian/Carboniferous transition). The entire studied succession has a thickness of about 600 m and was measured in cm scale. The base of the section is located at N 44° 21`56.6``, E 99°

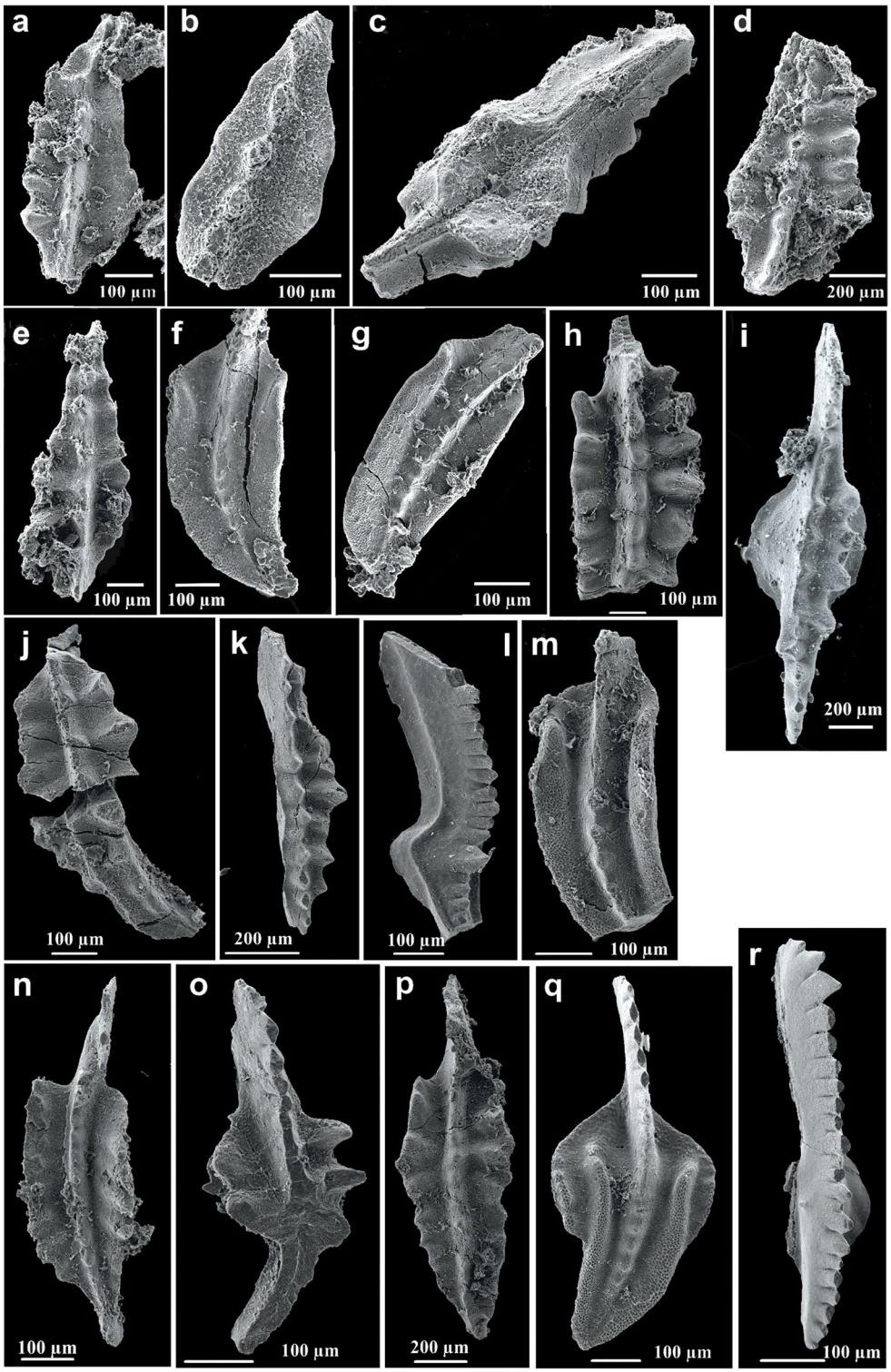


**Fig. 5:** Conodonts from the Indert Formation, and from the more detailed section in the east at the base of the formation (compare Fig. 3) **a** *Pseudopolygnathus* sp. (sample SHB-F/F-1); **b** *Polygnathus* sp. (sample SHB-F/F-1); **c, d** *Pseudopolygnathus primus* Branson and Mehl, 1934b (sample SHB-F/F-5); **e** *Pseudopolygnathus* cf. *primus* Branson and Mehl, 1934b (sample SHB-F/F-5); **f**, **g** *Polygnathus communis communis* Branson and Mehl, 1934b (sample SHB-F/F-5); **h** *Pseudopolygnathus* cf. *primus* Branson and Mehl, 1934b (sample SHB-F/F-3); **i** *Bispathodus aculeatus aculeatus* Branson and Mehl, 1934a (sample SHB-C-1), not typical as the posterior bar is wider as normal; **j** *Pseudopolygnathus primus* Branson and Mehl, 1934b (sample SHB-C-1); **k** *Bispathodus costatus* Branson, 1934 (sample SHB-C-3); **l** *Palmatolepis gracilis sigmoidalis* Ziegler, 1962 (sample SHB-C-3); **m** *Polygnathus communis communis* Branson and Mehl, 1934b (sample SHB-C-3); **n** *Polygnathus* cf. *inornatus* Branson and Mehl, 1934b (with a short posterior blade, sample SHB-C-3); **o** *Pseudopolygnathus* sp., deformed specimen (sample SHB-C-3); **p** *Pseudopolygnathus primus* Branson and Mehl, 1934b (sample SHB-C-3); **q** *Polygnathus vogesi* Ziegler, 1962 (sample SHB-C-16); **r** *Bispathodus stabilis* Branson and Mehl 1934a (sample SHB-C-16)

26`59.1`` at an elevation of 1933 m above sea-level. Due to outcrop situation, we shifted the geological record to the east or west where necessary (see Fig. 1c, d) to avoid large thrusts and folded parts. This guaranteed measurement of a ± continuous succession. Each shift of the section is indicated in the lithological columns (Fig. 8a–d). The end of the section is located at N 44° 22`12.3``, E 99° 32`08.9`` at an elevation of 2062 m above sea-level.

The section begins with the Chuluun Formation, which conformably overlies shales and volcanic rocks of the Tsakhir Formation. The lower part of the Chuluun Formation is represented by the Hurenboom Member, a 70 m thick

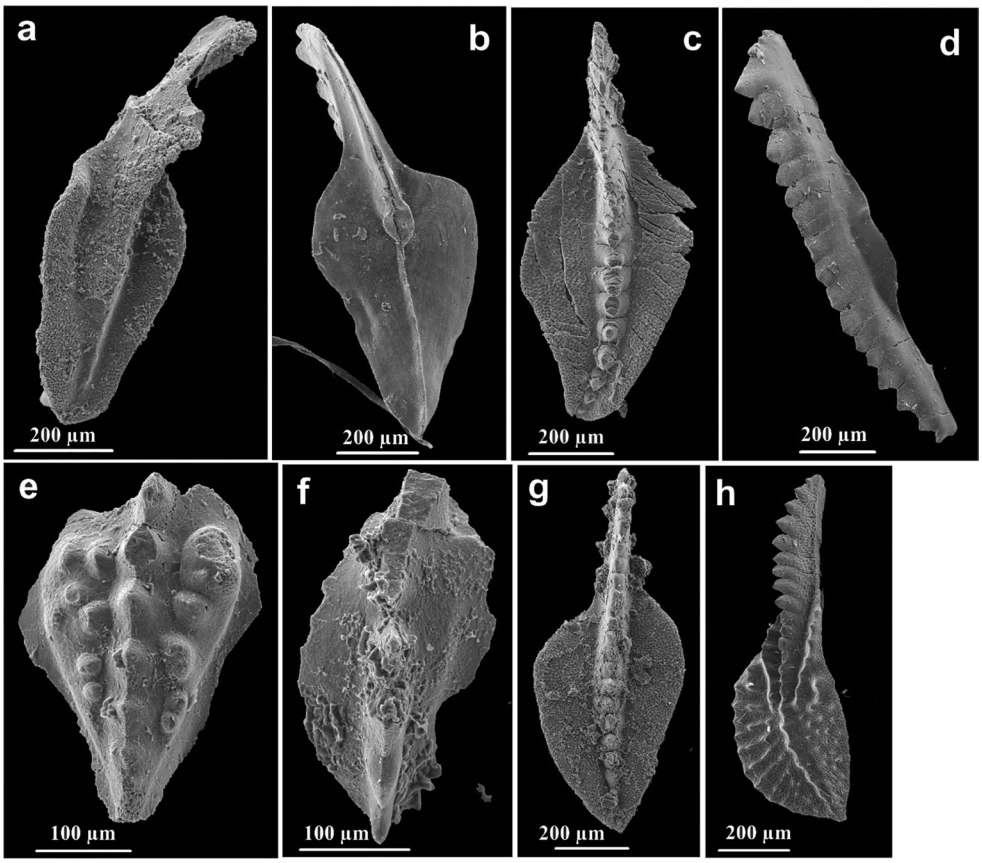


**Fig. 6:** Conodonts from the Indert Formation. **a** *Polygnathus communis communis* Branson and Mehl 1934a (sample SHB-C-33); **b** *Polygnathus purus purus* Voges 1959 (lower view, sample SHB-C-33); **c** *Polygnathus purus purus* Voges 1959 (upper view, sample SHB-C-33); **d** *Bispathodus stabilis* Branson and Mehl 1934a (sample SHB-C-38); **e** *Protognathodus kockeli* Bischoff, 1957 (sample SHB-C-38); **f** *Protognathodus* cf. *meischneri* Ziegler, 1969 (sample SHB-C-38); **g** *Polygnathus purus purus* Voges, 1959 (sample SHB-C-40); **h** *Siphonodella duplicata* Branson and Mehl, 1934b (Sample SHB-C-40)

limestone succession, which is composed of well-bedded biostromal limestones (Figs. 8a, 9a). These limestones were interpreted to represent a shallow-marine ramp environment (Pellegrini et al. 2012). Skeletal fragments are dominated by corals (e.g. solitary rugosans, thamnoporids, syringoporids), stromatoporoids and bryozoans. Brachiopods, bivalves, ostracods, and trilobites occur in low abundance, whereas crinoids are more frequent in distinct layers. The Hurenboom Member is characterised by skeletal wackestones and packstones, whereas framestones, bafflestones and boundstones occur in specific horizons and are less frequent.

The base of the section is composed of small domical and laminar stromatoporoids, and bioclastic wackestones. From about 5 m above the base more corals (solitary rugose, thamnoporids, and syringoporid corals) occur in association with bryozoans. More laminar and low-domical stromatoporoids show up at about 12 m from the base, which are overlain by thamnoporid bafflestones (Fig. 9b, c). 21 m from the base coral floatstones are covered by laminated stromatoporoids (up to 30 wide and 1-2 cm thick, Fig. 9d) and thin-bedded crinoidal grainstones, which alternate with domical stromatoporoids. Rare stratified thamnoporid biostromes as well as stromatoporid and coral boundstones, which have a size of about 60 cm in width and are 25 cm height, were observed in the section at about 32 m above the base. Those small-scaled biostromes were also described by Pellegrini et al. (2012) from the same section. The low-domical stromatoporoids and corals reappear from about 35 m to 38 m from the base (Fig. 8a). They do not exhibit wide lateral extension, they built small clusters instead. The surrounding sediment is composed of wackestones or lime mudstones. The overlying four metres are characterised by a fossil assemblage of corals, laminar stromatoporids, and bryozoans. A brecciated limestone occurs at 44 m above the base of the section (Fig. 8a, base of column b).

The next succession ranging from 43 m to 55 m exhibits a rich fauna, which is composed of bryozoans, laminar stromatoporoids and different corals, such as thamnoporids and solitary rugose corals in association with crinoidal grainstone in the upper part. These limestones are covered by a massflow deposit of about 60 cm thickness, which rests upon crinoidal grainstone (Fig. 9e). This unit is overlain by stratified thamnoporid biostromes associated with rugose corals (Fig. 9f, sample SH-S-8) and bryozoans. The overlying limestones exhibit a decrease in thamnoporid corals, and colonial corals become sparse while laminated stromatoporoids with rugose corals are more common. The top of the section is very similar in faunal composition as the base of the carbonate succession with laminar stromatoporids, thamnoporid and syringoporid corals,

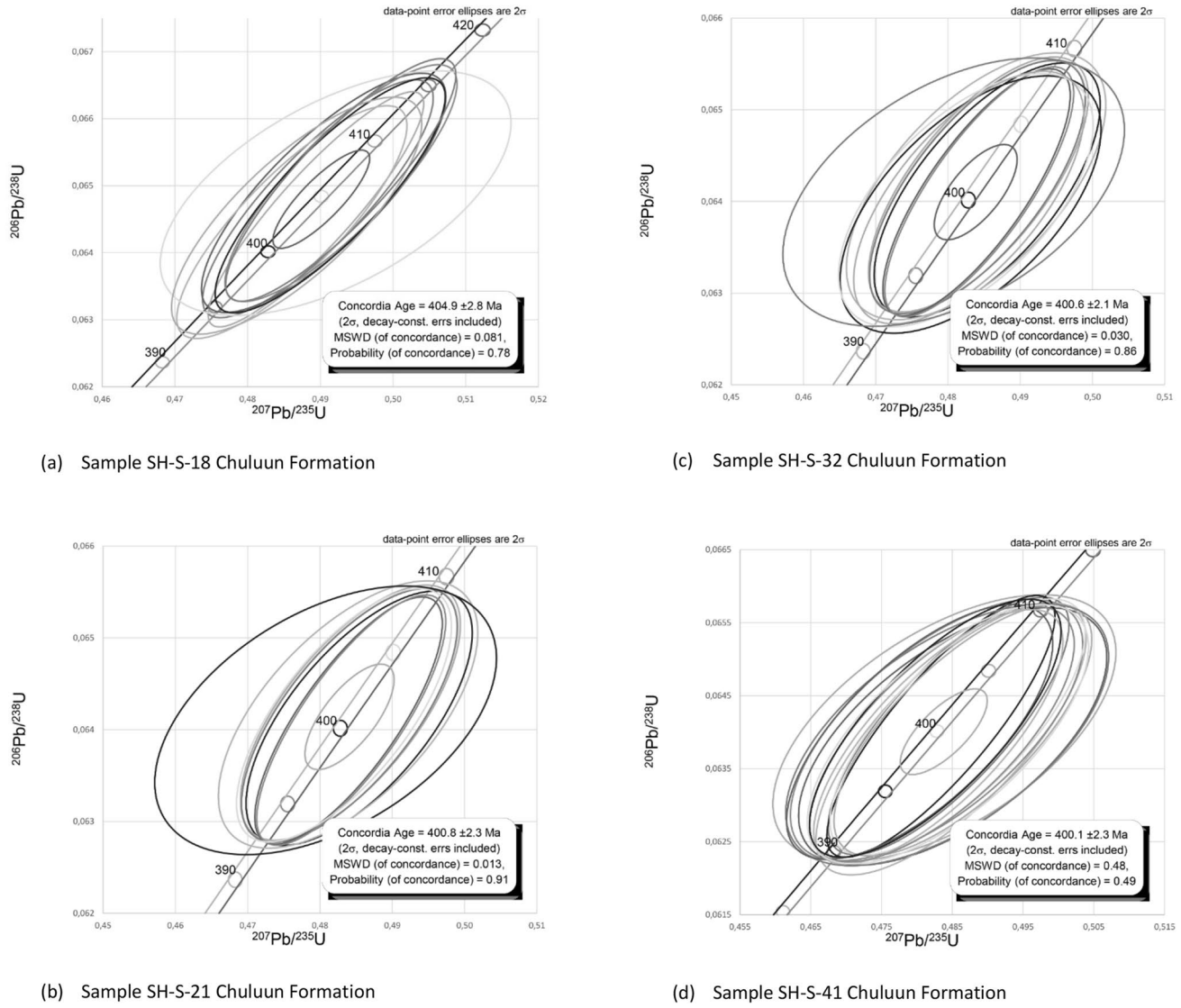


**Fig. 7:** Concordia age diagrams for samples of the Chuluun Formation, Carbonate-Volcanic Member, Shine Jinst (southern Mongolia)

associated with rare brachiopods and some bryozoans. In distinct layers (sample SH-S-15) characteristic floatstones (Fig. 9g) occur. Interestingly, there is neither a profound difference in average organism size, nor in changes of biodiversity patterns throughout the Hurenboom Member, which confirms data based on a detailed guild concept study by Pellegrini et al. (2012). The sedimentological record of the Hurenboom Member is rather homogeneous as no siliciclastic sediments are interbedded, no wave ripples occur and no evidence of intertidal deposits were found. Fundamental sedimentological differences are rare and occur in distinct layers, such as intercalated thin-bedded crinoidal grainstones. Two layers, which differ from the lithofacies described above are a thick limestone breccia (Fig. 8a, base of column "b") and a mass-flow deposit. The thicknesses of the single beds of the Hurenboom Member are more or less constant and vary between 15 cm to 35 cm and the fossil community is rather uniform and less divers.

The overlying Carbonate Volcanic Member of the Chuluun Formation starts with grey limestones, which are covered by an interval of greenish shales, tuffs, and greenish shales with limestone lenses (Fig. 8a). In the middle part of this succession, a thin-bedded black limestone occurs (sample SH-C-20, Fig. 8c). The following few metres are not well exposed. Between two covered intervals a limestone conglomerate occurs above a fossiliferous limestone. The conglomerate pebbles are mainly composed of limestones representing reworked material of underlying units. Rare pebbles of volcanic rocks occur as well, but they are less frequent. The following 14 m thick unit is composed of volcaniclastic rocks and thick-bedded andesitic basalts (sample SH-G-9). This succession is covered by grey

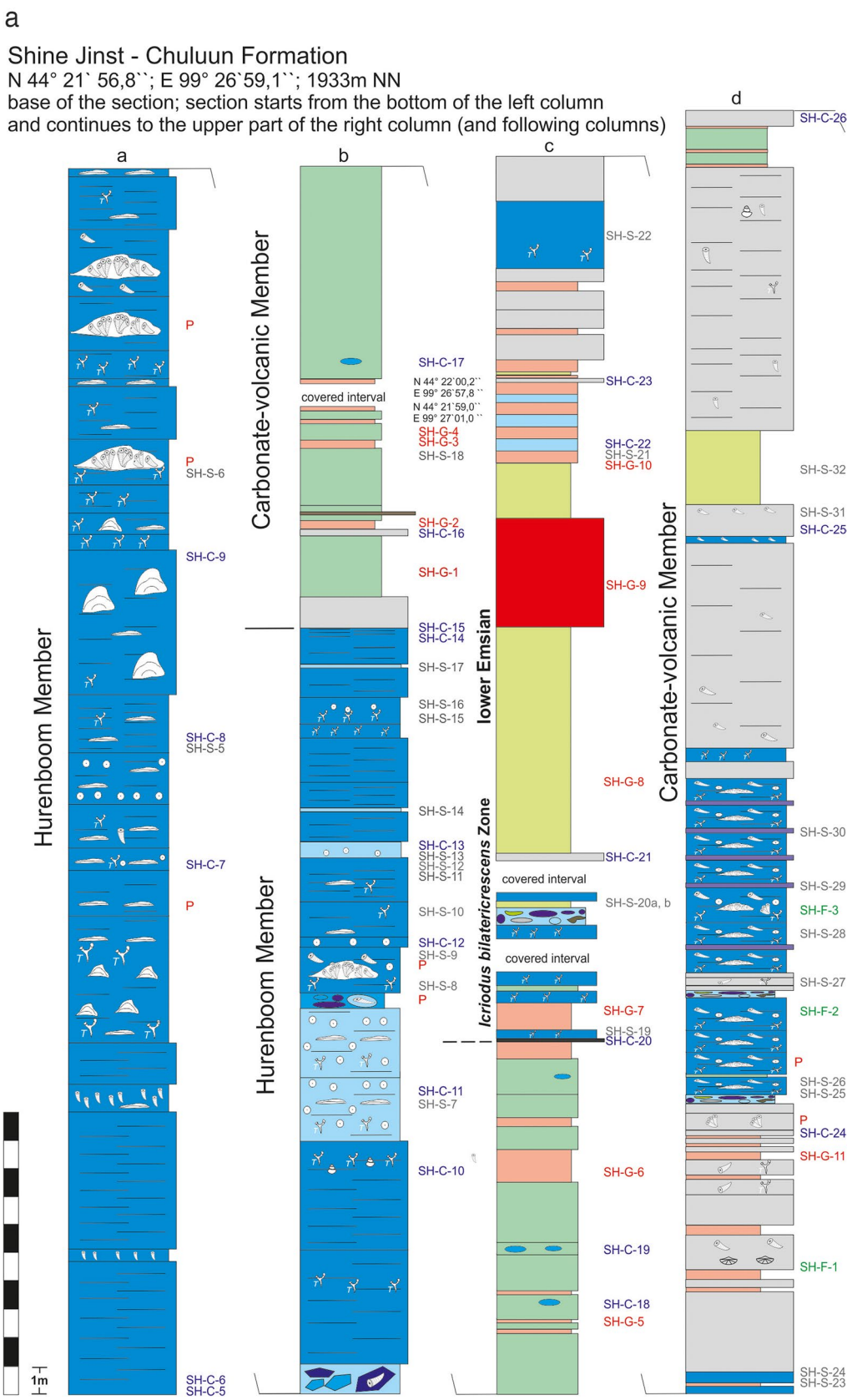


**Fig. 8 a:** Lithological log of the section

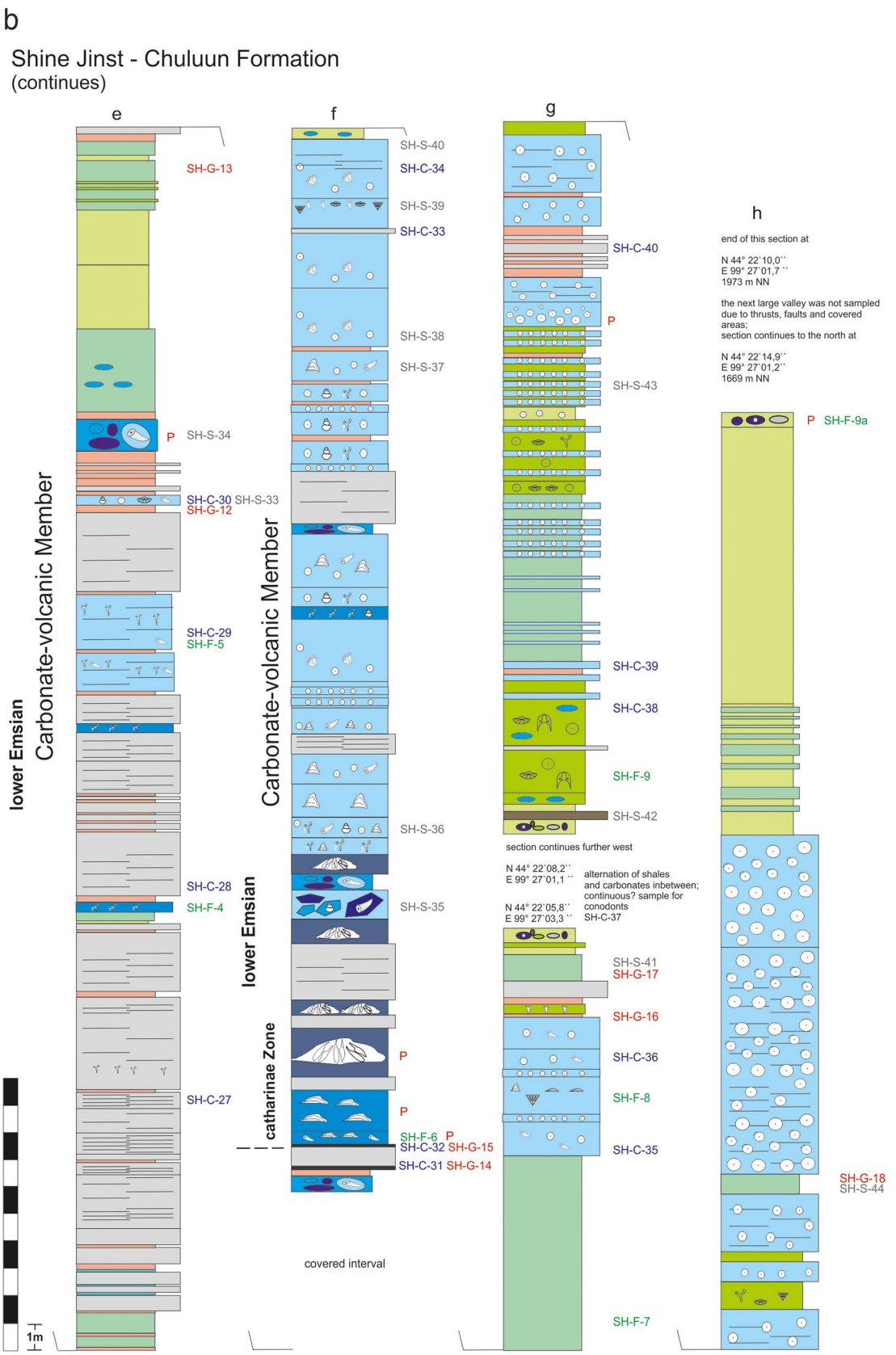


**Fig. 8 b:** Lithological log of the section

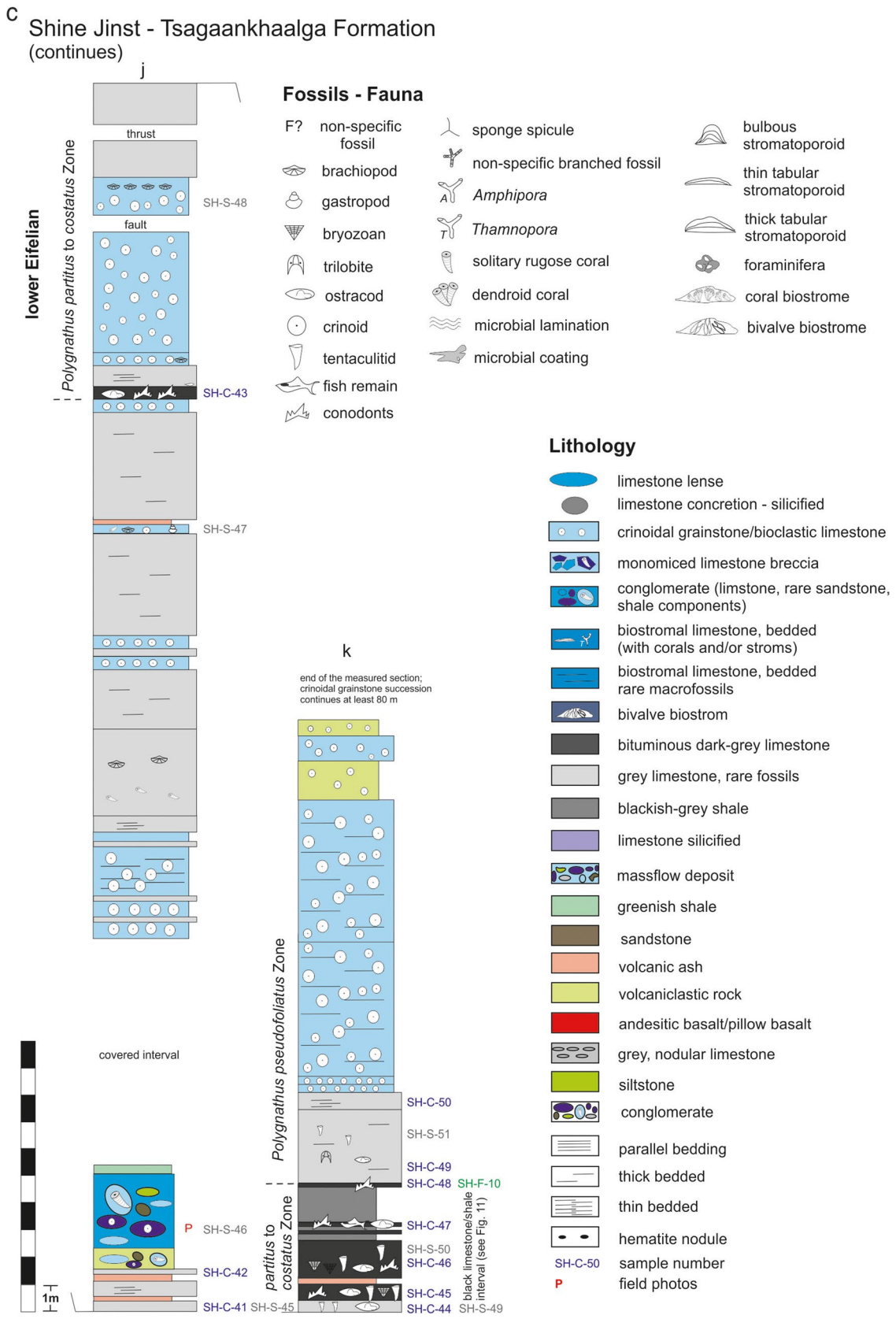


**Fig. 8 c:** Lithological log of the section

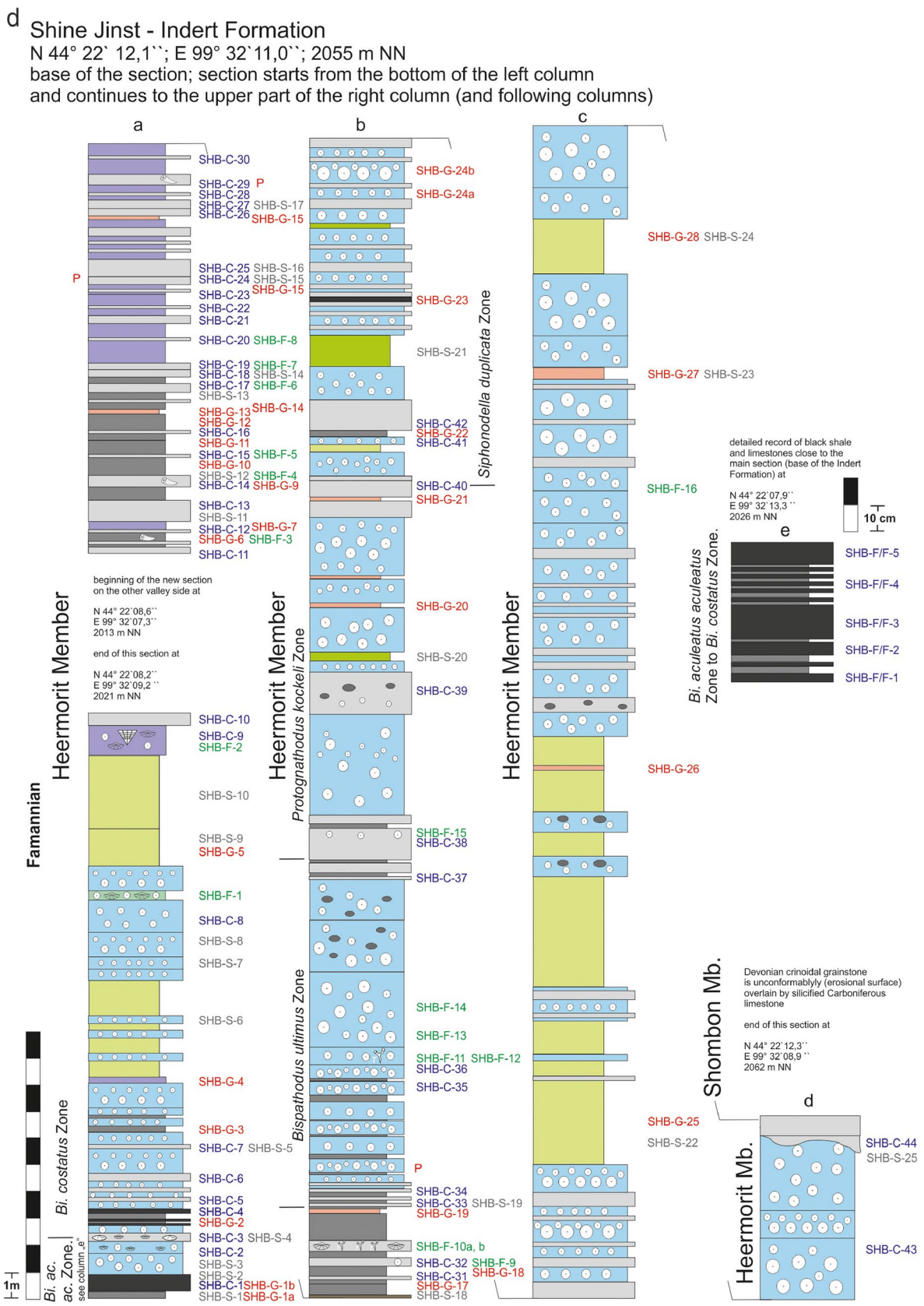


**Fig. 8 d:** Lithological log of the section

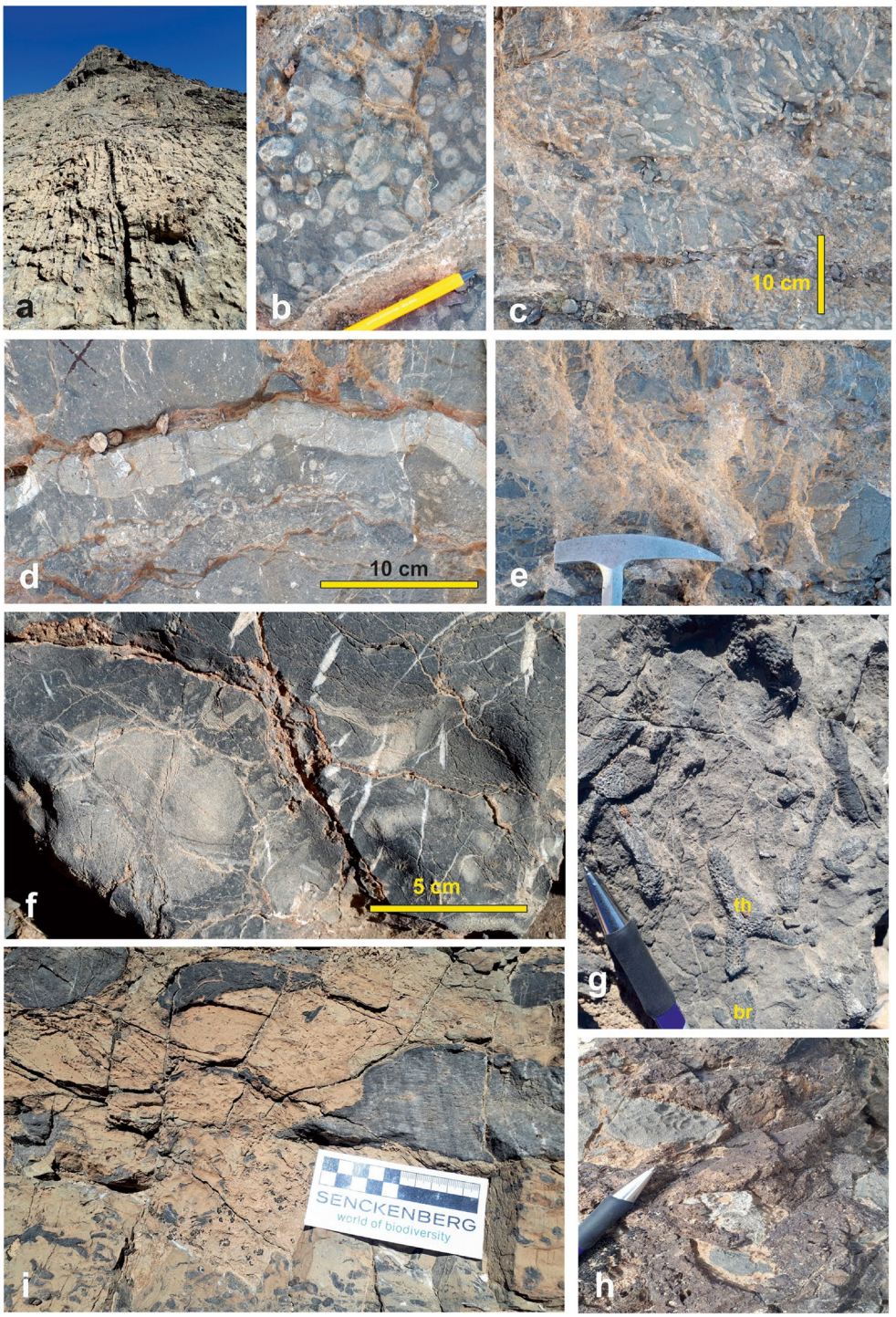


**Fig. 9:** Field photos showing sedimentological features and fauna (Chuluun Formation): **a** Prominent ridge of well-bedded biostromal limestone at the base of the Chuluun Formation; beds dipping to north-northeast at high angle, bedding thickness is roughly constant (15–35 cm). **b** Densely packed thamnoporid bafflestone in micritic matrix (pencil for scale). **c** Well-bedded thamnoporid floatstone (at the base) and bioclastic wackestone at the top (Hurenboom Member, Chuluun Formation). **d** Large laminar stromatoporoid covered by crinoidal grainstone below sample SH-C-7 (see Fig. 3). **e** Massflow deposit in the upper part of the Hurenboom Member, Chuluun Formation; the matrix between pebbles is a micritic limestone (hammer for scale). **f** Large rugose coral in a bioclastic wackestone. **g** Coral floatstone at the top of the Hurenboom Member (pencil for scale). **h** A polymict, deeply weathered limestone conglomerate from the Carbonate-Volcanic Member of the Chuluun Formation (Fig. 3, column e, sample SH-S-34). **i** Coral floatstone at the base is covered by low-domical, non-enveloping stromatoporoids in situ; this limestone is characterised by a fossiliferous micritic matrix and/or a lime mud matrix (Carbonate-Volcanic Member, sample SH-F-6)

limestones with less fossils and some tuffs until the lower part of column "d" (Fig. 8a). Lithofacies changes again with a thin-bedded limestone conglomerate (sample SH-S-25), similar to that described above. The overlying unit is composed of stromatoporoid/coral biostromal limestones. Faunal diversity is low, and low-domical stromatoporoids occur in micritc matrix. Bioclasts are rare and mainly composed of brachiopods and bryozoans. The cyclic succession of coral floatstones, which are overlain by stromatoporoids is repeated several times (Fig. 8a, column "d") and the entire interval has a thickness of about 13 m. Intercalated is a conglomerate, which is covered by grey limestones with rare fossils. The overlying interval of about 54 m is composed of grey limestones with rare fossils, intercalated volcanic rocks, greenish shales, and bioclastic limestones in the upper part (Fig. 8a; Fig 8b, column "e").

This succession is overlain by a mixture of volcaniclastic rocks, a polymict 1.30 m thick carbonate conglomerate (Fig. 8h, sample SH-S-34), shales with limestone lenses, and a grey limestone at the top. Based on conodont data this conglomerate occurs within the *bilatericrescens bilatericrescens* Zone. The not exposed 6 m thick interval at the base of column "f" (Fig. 8b) is covered by a 30 cm thick limestone conglomerate with a similar pebble composition described before (sample SH-S-25), which is overlain by a volcanic ash. A grey limestone is intercalated between two thin-bedded Emsian black limestones (samples SH-C-31 and SH-C-32).

The limestones are overlain by low-domical stromatoporoids as described before (see Fig. 9i). Above sample SH-F-6, a similar succession occurs between sample SH-S-26 and SH-S-30 (Fig. 8a, column "d"). The following 6 m thick interval is represented by an alternation of grey limestones and biostromal limestones. These limestones contain rare but large macrofossils and are unique. They are composed of large bivalves in live position. The length of the shells exceeded 15 cm (Fig. 10a) and average 7–10 cm. The shells are mainly compressed in dorsal-ventral direction and are elongated in the anterior-posterior direction. The posterior half of the shells consist of a wing-like flat flanges (Fig. 10b). Single bivalve biostromes (Fig. 10c) reach a height of 30 to 50 cm and a lateral extension of up to 2 m. The bivalve biostromes occur in four distinct horizons (Fig. 10b, column "f") and can be mapped for several decimetres laterally. Micrite filled the spaces between the large shells. The bivalves may belong to the family Alatoconchidae or Megalodontids (pers. com. Krzysztof Hryniewicz, Polish Academy of Sciences; work in progress). The third bivalve biostrome is overlain by a polymict limestone breccia (sample SH-S-35), which is covered by a limestone conglomerate. Fragments of the breccia and pebbles of the conglomerate contain different limestone types, such as bioclastic limestone, grey limestone and bivalve shells of underlying rocks. The conglomerate is overlain by the fourth bivalve biostrome horizon.

The following 26 m thick unit is mainly composed of bioclastic limestones, crinoidal limestones, and less-fossiliferous grey limestones. Intercalated are thin-bedded ash layers. The overall fossil community is rather uniform and less diverse but in distinct layers fish remains occur. In one horizon of the Chuluun Formation some vertebrate remains occur along with a remarkable large remnant of an articulated Early Devonian fish (according to the conodont record this succession occurs in the *catharinae* Zone), which was found above the fourth bivalve biostrome (Fig. 8b, column "f", Fig. 10d). According to Martin Brazeau (UK pers. com.) the fish remain looks like a chondrichthyan/acanthodian of some sort, viewed from the internal side of the scale bases and the crowns cut through. It could be *Altholepis* or *Polymerolepis*, or something similar, which is even more interesting, as those are extremely rare anywhere in the world.

At the top of this succession volcaniclastic rocks with reworked limestone pebbles occur (Fig. 8b, top of column "f"). The next 16 m of the section are characterised by a thick succession of greenish shales, bioclastic limestones, crinoidal grainstones, grey limestones, siltstones, and a conglomerate at the top. The matrix of this conglomerate is composed of volcaniclastic material, which terminated the shallow-water carbonate sedimentation for a while during the late Emsian.

The section continues further west (see Fig. 1c) with the conglomerate marker horizon at the base (Fig. 7b, column g), which is overlain by an immature sandstone (sample SH-S-42) and volcaniclastic rocks. The following 18 m thick succession is composed of alternating fossiliferous siltstone with carbonate lenses, greenish shales, and crinoidal grainstones. Intercalated are volcaniclastic rocks, which contain reworked crinoids. This succession is conformably overlain by thick-bedded crinoidal grainstones to packstones. While most thin-bedded crinoidal grainstones exhibit graded bedding and totally disarticulated crinoid stems, thick-bedded beds are generally poorly sorted and contain large crinoid stems in a sparitic matrix (Fig. 10e, sample SH-S-43). Distinct layers exhibit invers gradation. Crinoidal grainstone to packstone made of 65-80% of crinoidal fragments along with rare dissociated brachiopod shells, rugose and tabulate corals and bryozoans. Intergranular porosity is rare and filled by sparite. The next 26 m thick interval is dominated by crinoidal grainstones to packstones as described before with intercalations of siltstones, ash layers, and grey limestones. This unit is covered by 16 m thick succession of volcaniclastic rocks and intercalated shales at the basal part. The top of this unit is covered by a conglomerate (Fig. 8b, column "h", sample SH-F-9a). Due to the complex tectonic situation and a thick sedimentary cover ("Chuluun Valley Member" in Fig. 1c) we continued measuring of the section further to the northwest, starting with an alternation of grey limestones and tuffs at the base (Fig. 8c, column "j"). These rocks are conformably overlain by a 3.60 m thick conglomerate, which is mainly composed of different limestone pebbles, less common are sandstones and shales. The sizes of the pebbles vary from 2 cm to 16 cm in diameter (Fig. 10f). At the base, the matrix is composed of volcaniclastic material (Fig. 10g), whereas the matrix of the upper part of this conglomerate is represented by lime mudstones to wackestones (sample SH-S-46). According to Wang et al. (2005b) the Tsagaankhaalga Formation starts with a conglomerate and is of lower Eifelian.

This succession is covered by green shales. The section continues 32 m upon a covered interval of approximately 10 m and is characterised by an alternation of crinoidal

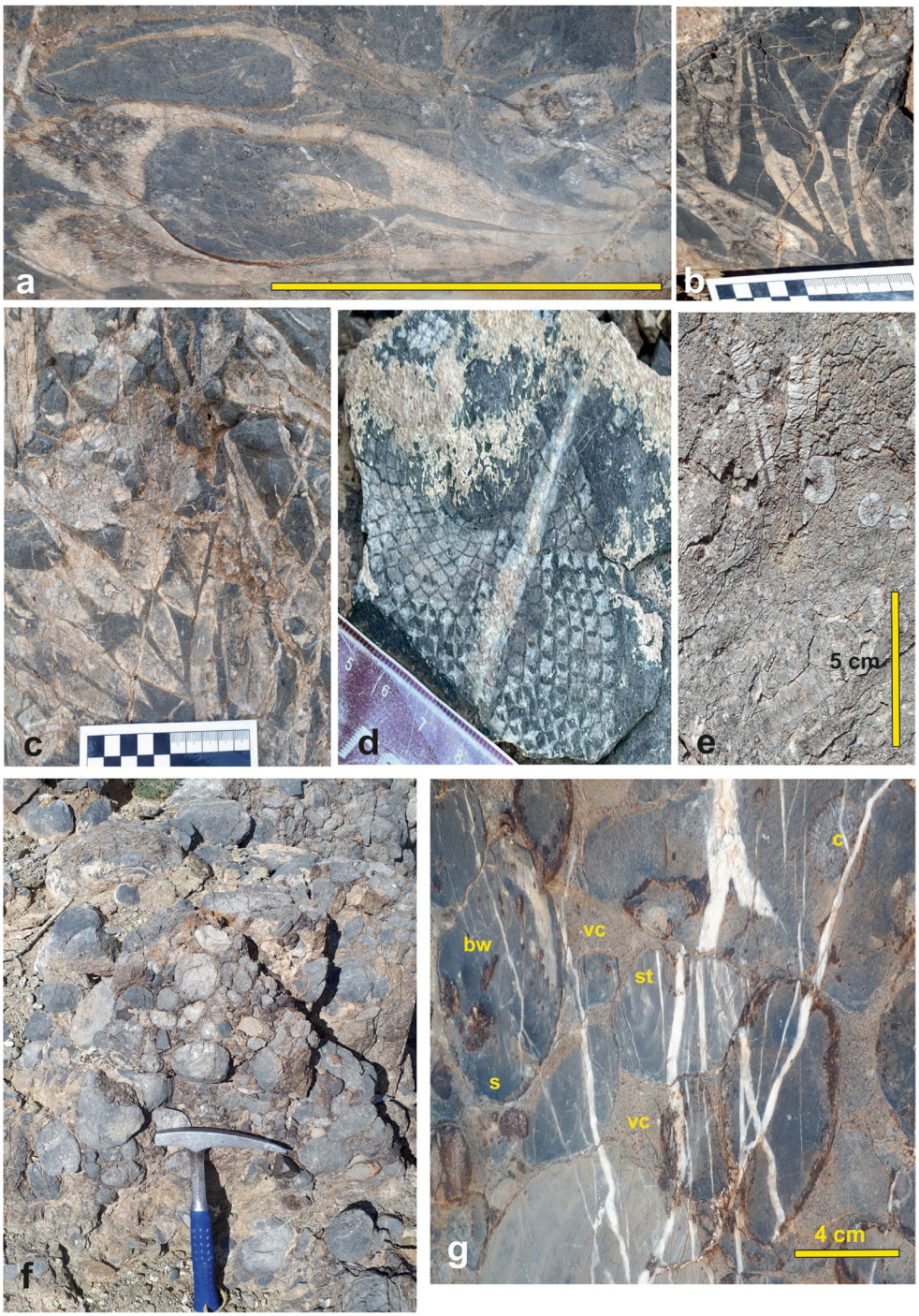


**Fig. 10:** Field photos showing sedimentological features and fauna. **a** Giant bivalve shells in situ (scale = 10 cm). **b** The posterior half of the shells consist of a wing-like flat flanges on each valve. **c** Bivalve biostrome belonging to ?Alatoconchidae or Megalodontids from the Carbonate-Volcanic Member of the Chuluun Formation. **d** Large fish remain of ?*Altholepis* or ?*Polymerolepis*, from the Carbonate-Volcanic Member of the Chuluun Formation, above the bivalve biostrom. **e** Poorly sorted crinoidal grainstone to packstone with large stem fragments (Tsagaankhaalga Formation above sample SH-S-43). **f** A polymict conglomerate with large cobbles of different sizes. The matrix is composed of volcaniclastic material (hammer for scale). **g** Detail of the conglomerate: *bw* bioclastic wackesteone, *st* domical stromatoporoid, *c* tabulate coral, *vc* volcaniclastic matrix

limestones (similar as described above), grey, massive limestones with small corals, brachiopods, and ostracods. Intercalated is a dark-grey, lower Eifelian limestone (sample SH-C-43). In the upper part of this succession a small-scaled thrust was mapped (Fig. 8c). This interval is overlain by dark-grey limestones and blackish-grey shales (limestone/shale interval, see Fig. 11). The bituminous limestones yielded conodonts suggesting an early Eifelian age (see section biostratigraphy), which includes rocks representing the Choteč Event. This unit is covered by grey limestones and thick-bedded crinoidal grainstones. The latter ones exhibit the same microfacies characteristics as described before. Very thick-bedded layers show hummocky cross-stratification and contain large stem fragments (grainstone to packstone), thin-bedded layers are characterised by rather small disarticulated crionoid columnals, often showing graded bedding. At the end of this measured section two thick-bedded volcaniclastic rock occur, which contain reworked crinoids.


**Fig. 11:** Field photo showing the Tsagaankhaalga Formation, Shine Jinst (compare Fig. 8c, column "j" to "k") with black shales and limestones, which represent equivalents of the Choteč Event

The next youngest succession starts at the base of the Indert Formation, which conformably overlies the Givetian (Sullivan et al. 2016) Gobi-Altai Formation. The latter one is subdivided into the lower Tentaculite Member and the upper Khar Member. The less fossiliferous Gobi-Altai Formation is characterised by sandstone, andesitic basalt, rhyolite, tuff, chert, and rare intercalated thin-bedded limestone layers (Minjin et al. 2001). The overall succession of this formation is very similar to the Minjin Member of the Botuulkhudag Formation further in the southeast (Mandalovoo Terrane, see Munkhjargal et al. 2021) and represent more deeper water environments. The Gobi-Altai Formation was not the focus of this study although we took some spot samples (fauna and biostratigraphy). As this is work in progress results will be published separately.

Our measured section of the Indert Formation starts with dark-grey shales and limestones, which seems to be incomplete due to small-scaled thrusts. Thus, a more complete succession of those blackish limestone and shale was mapped further to the east (see Fig. 8d, Indert Formation, column "e"). Interestingly, the Indert Formation in our section begins within the Famennian which means that we have no Frasnian rock record. The boundary to the underlying Gobi Altai Formation is difficult to define as the stratigraphic range of this formation is still unclear. According to Minjin et al. (2001) the Gobi Altai Formation has a stratigraphical range from the Givetian to early Famennian, which is not confirmed so far. In case the stratigraphic range of these authors is correct, a hiatus of several conodont zones is obvious as our section begins in the late Famennian. Even a larger hiatus seems possible based on the biostratigraphic studies provided by Sullivan et al. (2016). The bituminous black limestone and shale succession at the beginning of the section (see Fig. 8d) yielded a conodont fauna which points to the Dasberg Crisis. These sediments have a stratigraphical range from the Upper Devonian *Palmatolepis gracilis expansa* Zone to the *Bispathodus aculeatus aculeatus* Zone. Overlying rocks represent an alternation of crinoidal limestones and volcaniclastic rocks with intercalations of grey limestones and silicified bioclastic limestones. The following succession on the other side of a small valley is composed of an alternation of grey limestones, shales, and silicified limestones (Fig. 8d, Indert Formation, column "a"). The conodont record is good. We could define several conodont zones and trace the Hangenberg Event higher in this succession. At the lower part of the section (Fig. 8d) rocks are dominated by crinoidal grainstones with rare intercalations of grey and green shales, grey limestones, and volcaniclastic rocks. The crinoidal grainstones are composed of densely packed crinoid columnals, which reach several cm in length. The overall microfacies of crinoidal limestones is similar to that described from the Chuluun Formation (Carbonate Volcanic Member). Carbonate mud is rare and columnals are generally cemented by syntaxial calcite. Crinoid ossicles also occur within bioclastic wackestones and marly limestones but to a minor percentage, and are admixed with other skeletal grains. Some crinoidal grainstones exhibit graded bedding and thick-bedded layers show hummocky cross-stratification. Intercalated in this succession are thick-bedded volcaniclastic rocks, which are covered by silicified limestones and greyish, less fossiliferous limestones (Fig. 8d, column "a", Fig. 12a).

In the middle part of the Heermorit Member (late Famennian age) the overall facies setting changes and hemipelagic conditions prevail. This succession is also characterised by cyclic sedimentation, very similar to coeval sediments in southern Gobi (Munkhjargal et al. 2021b). Overlying rocks of about 20 metres are composed

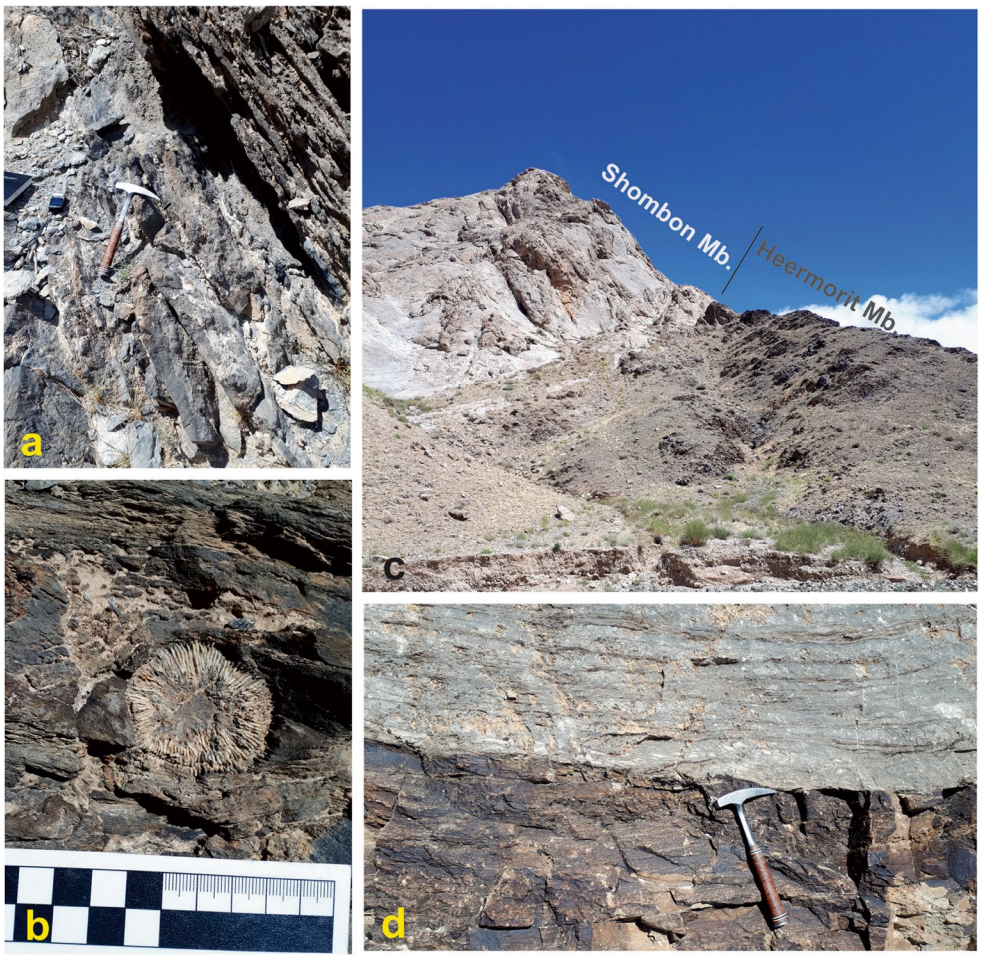


**Fig. 12:** Field photos from the Indert Formation. **a** Dark grey shales and limestones of the Indert Formation at the base, hammer for scale. **b** Large tabulate corals occur in calcareous shales of the in the Heermorit Member. **c** Sampled section of the Indert Formation; dark coloured rock of the Heermorit Member is covered by light grey rock of the Shombon Member. **d** Hammer marks the erosional contact between the Heermorit Member and the Shombon Member of the Indert Formation

of an alternation of greyish limestones, shales with large isolated corals (Fig. 12b), and silicified limestones. Intercalated are several thin-bedded ash layers. The middle part of the Heermorit Member most likely contains the D/C boundary, which is proven by the conodont record (see chapter on biostratigraphy). The next 45 metres are dominated by crinoidal grainstone as described before. Some beds can reach thicknesses of up to 3 m. Intercalated in this succession are less fossiliferous limestones, siltstones and rare thin-bedded volcaniclastic rocks. In the upper part, a several cm thick black shale occurs (sample (SHB-G-23). These rocks are overlain by a 15 m thick succession of volcaniclastic rocks with rare crinoidal grainstone layers (see Fig. 8d, column c). The overlying sequence until the top of the section is again dominated by crinoidal grainstone as before. Rocks of the Heermorit Member and the Shomboon Member exhibit fundamental lithological differences (Fig. 12c). Whereas the first member is mainly composed of crinoidal grainstone, the second one is characterised by less fossiliferous grey limestones, which unconformably overlie the older member (Fig. 12d). The transition marks the end of our measured section within the Carboniferous.

## Discussion

The study area is characterised by variable shallow-water sedimentation with rare intercalations of hemipelagic sedimentation during the Middle Devonian (e.g. basalts of the Gobi Altai Formation) and the late Famennian. The entire succession is associated with strong volcanism and tectonics. One of the most important transitions from preferably calcareous platform deposition to active tectonics occurred during the Lochkovian to Pragian stages of the Early Devonian, were alluvial-fan deposits, unconformities, and volcanism suggest syndepositional tectonism and coeval volcanic activity. Gibson et al. (2013) introduced the term "Tsakhir Event". This event is documented by a major regression, which finally led to the deposition of several metres-thick conglomerates at the base of the Tsakhir Formation. This event is assumed to be regional, rather than globally significant in terms of eustatic sea-level changes. Coeval rocks in Southern West Siberia and Australia do not provide evidence of a major regression at that time (Talent and Yolkin 1987). Reef building organisms in the studied section were affected by this regression, which led to a profound change of reef communities. The Early

Devonian unconformity, which is present in the Trans-Altai and in the Gobi-Altai zones is related to the formation of an Early–Middle Devonian arc in the Edrengin and Dzolen subzones (Fig. 1a) and back-arc volcanism in the northern Khuvinkharin Subzone that developed on a passive margin succession of the Trans-Altai Silurian-Devonian oceanic basin (Lehmann et al. 2010).

The measured section starts with the Hurenboom Member of the Chuluun Formation, which exhibits a rather uniform lithofacies. Main rocktypes are skeletal wackestones and packstones, whereas floatstones, bafflestones, and boundstones occur in distinct layers and represent environmental changes, which were most likely linked with variable wave or current energy. Two layers, which differ from the lithofacies mentioned above are a thick limestone breccia and a mass-flow deposit. The clast-supported monomict limestone breccia is interpreted as mass-flow breccia resulting from submarine slides of semi-consolidated sediments triggered by synsedimentary tectonic activity and/or earthquakes (see similar successions described by Böhm et al. 1995).

Reef-building organisms of the Hurenboom Member reveal a rather unique community, which does definitely not represent a real reef as proposed by Alekseyeva (1993) and later adopted by Kröner et al. (2010), as reefs require laterally confined, three-dimensional features raising significantly above the sea floor. Two-dimensional features of skeletal builders grown on a single horizontal bedding surface, lacking cavity spaces, cements and cryptic and encrusting biota are described as biostromes (e.g. stratified biostrome). Reef building organisms, such as colonial corals and stromatoporoids are in life position and occur mainly in a micritic matrix (see e.g. MacNeil and Jones 2016), but they exhibit limited vertical growth and lateral extension of individuals. Stromatoporoid morphology and sediment matrix point to slightly deeper water conditions, which is consistent with the facies model of James and Bourque (1992). The low density and low abundance of reef builders confirm that the bioconstructors of the studied section failed to create a real reef (Pellegrini et al. 2012), although potential reef-building organisms were present. From the palaeogeographic viewpoint, southern Mongolia was located at 30–35° latitude in the Early Devonian and also the assumed water-temperatures of about 30°C (e.g. Copper and Scotese 2003) should have been suitable to establish real reefs. Stromatoporoid/coral reefs occur in the Early Devonian in comparable latitudes such as in South China and in the Urals (Antoshkina and Königshof 2008; Shen et al. 2008). Colonization took place on the drowned platform in the Shine Jinst region (beginning of the section upon the shales of the Tsakhir Formation, which might be linked with a global transgression at the beginning of cycle Ib; see Johnson et al. 1985, Brett et al. 2011), but reef builders never reached high enough density to exceed initial reef development. They form rather isolated clusters instead, which show up as scattered low-domical stromatoporoids, or coral biostromes, and they occur in distinct layers. Hypothesis are presented by Pellegrini et al. (2012) and there might be several reasons, which are most likely responsible for hampering the establishment of real reefs in the Shine Jinst region during the Early Devonian. Unsuitable or unstable substrate precluded organisms from expanding laterally, e.g. hard substrate is limited, such as shell beds, crinoidal grainstone etc. and may have hindered organismal growth. In comparison to other sections such as in the Rhenish Massif this aspect might not be the main limiting factor as stromatoporoids developed preferably on mudstone or reworked volcaniclastic material, which finally led to the development of real reefs of different sizes (Königshof and Flick in press; Königshof et al. in press a, in press b). The bedding thicknesses of limestones of the Hurenboom Member are more or less constant (15 to 35 cm, Fig. 9a), suggesting that accommodation space remains uniform (balance of subsidence and sedimentation rates) and may have hampered vertical growth. The isolated position of the Shine Jinst region between an unknown continent and a volcanic arc in the Early Devonian (Badarch et al. 2002; Lamb et al. 2008; Gibson 2010) where the shallow-marine carbonate ramp evolved, might be another reason for the unsuccessful colonization. Similar features are known from an intra-oceanic island arc in Australia were in situ globular stromatoporoids grew as scattered colonies on skeletal sands forming less densely populated biostromes, which never accumulated enough to build a real reef (Pohler 1998). Underwood et al. (2009) has shown that geographic isolation may result in less successful colonisation because of the dispersal limits of planktonic larvae. Endemic faunas, which were reported from adjacent regions (Cronier et al. 2021; Nazik et al. 2021; Roelofs et al., 2021; Waters et al. 2021) may support this hypothesis. Endemic species are known from this section too, e.g. conodonts and ostracods. On the other hand, it seems likely that the CAOB was a biodiversity hotspot for bryozoans and echinoderms (e.g. Webster 2003; Waters et al. 2021, 2023). Finally, facies development in the Shine Jinst region exhibits a fundamental break in the carbonate platform evolution in the Early Devonian as reef communities were affected by a major regression and deposition of several metres-thick conglomerates at the base of the Tsakhir Formation (Gibson et al. 2013). This event obviously resulted in a fundamental change of the carbonate factory. As it was discussed by Stearn (2001) and May and Rodriguez (2012) a general decline at the end of the Silurian and the long-lasting recovery might be another limiting factor and/or unsuitable substrate to establish biostromes (Antoshkina and Königshof 2008). Although corals occur, they are isolated (Fig. 9f) and don`t have a wide lateral expansion, similar to stromatoporoids described above.

The Hurenboom Member is conformably overlain by the Carbonate Volcanic Member, which marks the beginning

of a very variable sedimentological/facies development. Biostratigraphic data and some geochronological results from the Chuluun Formation confirm an Emsian age. Whether this formation also ranges into the Eifelian (e.g. Wang 2005b) remains questionable due to limited conodont data in the upper part of this formation. Volcanism increases and carbonate sedimentation generally differs from previous limestone successions as described above, but the succession contains inimitable units. The large bivalves found in the section (Fig. 10a–c) may belong to the family Alatoconchids. Alatoconchids were once grouped into reef builders or biostrome builders (Kiessling and Flügel 2000) and they occur worldwide. They are reported from South China, Thailand, Phillippines, and Alaska (Kiessling and Flügel 2000; Blodgett and Isozaki 2013; Udchachon et al. 2014; Chen et al. 2018). The wide, wing-like flanges of the shells are most likely an adaptation to life on a soft sediment surface, which fits to the environment of the studied section. Micritic limestones and rare wackestones filled in the spaces between the large shells (Fig. 6b–d), which suggests low-energy conditions (Chen et al. 2018; Yancey and Boyd 1983). The flat shells are usually stacked and compacted tightly (Fig. 10c, d). According to Chen et al. (2018) the habitat of the giant clams was a setting of normal marine salinity and warm water, in the lower part of the euphotic zone. The palaeogeographic position of approximately 35° N of the equator (Copper and Scotese 2003) and average sea surface temperatures around 30°C in the Early Devonian (Copper 2002) fit very well, but the known stratigraphic distribution of the Alatoconchid family is limited so far to the Permian (Kungurian to Capitanian; see Chen et al. 2018 cum lit.). The found specimens may represent precursors (work in progress), which would document the oldest record of Alatoconchids found in the world.

The occurrence of conglomerates in the Shine Jinst section is not restricted to the Lochkovian to Pragian interval, but occurs also in the Emsian. This conglomerate most probably represents a tectonically induced regression and siliciclastic sedimentation terminated the shallow-water carbonate sedimentation (lower part of the Chuluun Formation) during the late Emsian for a short period. This conglomerate with a volcaniclastic matrix is interpreted as a braided fluvial or fan delta deposit, which is similar with the conglomerate at the base of the Tsakir Formation. Marine sedimentation started again with the deposition of an immature sandstone, which is covered by fossiliferous shales and crinoidal grainstone in the upper part of the Chuluun Formation.

Another thick-bedded conglomerate of several metres thicknesses occurs at the base of the Eifelian (Tsagaankhaalga Formation, Wang et al. 2005a), which is also interpreted to represent braided fluvial or fan-delta (due to the large lateral extension) to shallow-marine deposits. A steep relief associated with uplift and volcanism (see volcaniclastic matrix of conglomerates at the base) might be a hypothesis for deposition of these sediments. This major regressive event in the Shine Jinst region, expressed as an unconformity as rapid transition of shallow marine carbonates of the Chuluun Formation and the coarse clastics (conglomerate) of the overlying Tsagaankhaalga Formation. The upper part of this conglomerate exhibits a calcareous matrix with remnants of marine organisms which may suggest an environmental chance from non-marine to marine sedimentation. This could be related to eustatic sea-level rise at the end of cycle Ib (Johnson et al. 1985, Brett et al. 2011), which is just a working hypothesis as detailed biostratigraphical control is not present so far although some new biostratigraphic data are presented in this report (see above). Several smaller-scaled conglomerates occurring in the measured succession may represent sediment emplacement by gravity flows during flood events and/or are associated with storm events in an overall shallow-water facies setting. Interestingly, the stratigraphical position of a thick conglomerate at the base of the Tsagaankhaalga Formation (Eifelian) is comparable to similar conglomerates of several metres thicknesses of the Eifelian Takhuul Member (Botuulkhudag Formation) described from the Mandalovoo Terrane (Bayankhoshuu Ruins section; Fig. 13) in southern Mongolia (Munkhjargal et al. 2021b).

Conodonts found in the Tsagaankhaalga Formation, the occurrence of large numbers of dacryoconarids in several samples point to equivalents of the Choteč Event, which is described for the first time from Mongolia. Also the Indert Formation starts in our record with event layers, namely the Dasberg Crisis. The two sampled sections exhibit the same stratigraphy based on conodont data (see above). Silicified limestones in the Upper Devonian are covered by crinoidal grainstones, which are the dominant rock type in the Famennian of the Shine Jinst section. Intercalated are volcaniclastic rocks. Crinoid grainstones are characterised by large crinoid stems, well-preserved crinoid columnals and poor sorting indicating in place degradation or deposition subsequent to transport, which is proven by syntaxial rim cement. Graded bedding may be associated with downward transport from an outer carbonate ramp setting by submarine currents. Hummocky cross-stratification indicate deposition during storm events, whereas slightly changes in microfacies of grainstones are explained by hydrodynamic changes on the deposition area (e.g. rise and fall of sea level). Deposition of massive crinoidal grainstones in our section are thought to have taken place between the fair-weather wave base and the storm wave base. Similar interpretations are reported from Europe (e.g. Waters and Sevastopulo 1984; Webster 2003; Debout and Denayer 2018) and America (Aussich 1999). This characteristic limestone was included by Wilson (1975) in SMF 12.

The remarkable thicknesses of these sediments point to a relatively long-lasting stable environmental conditions

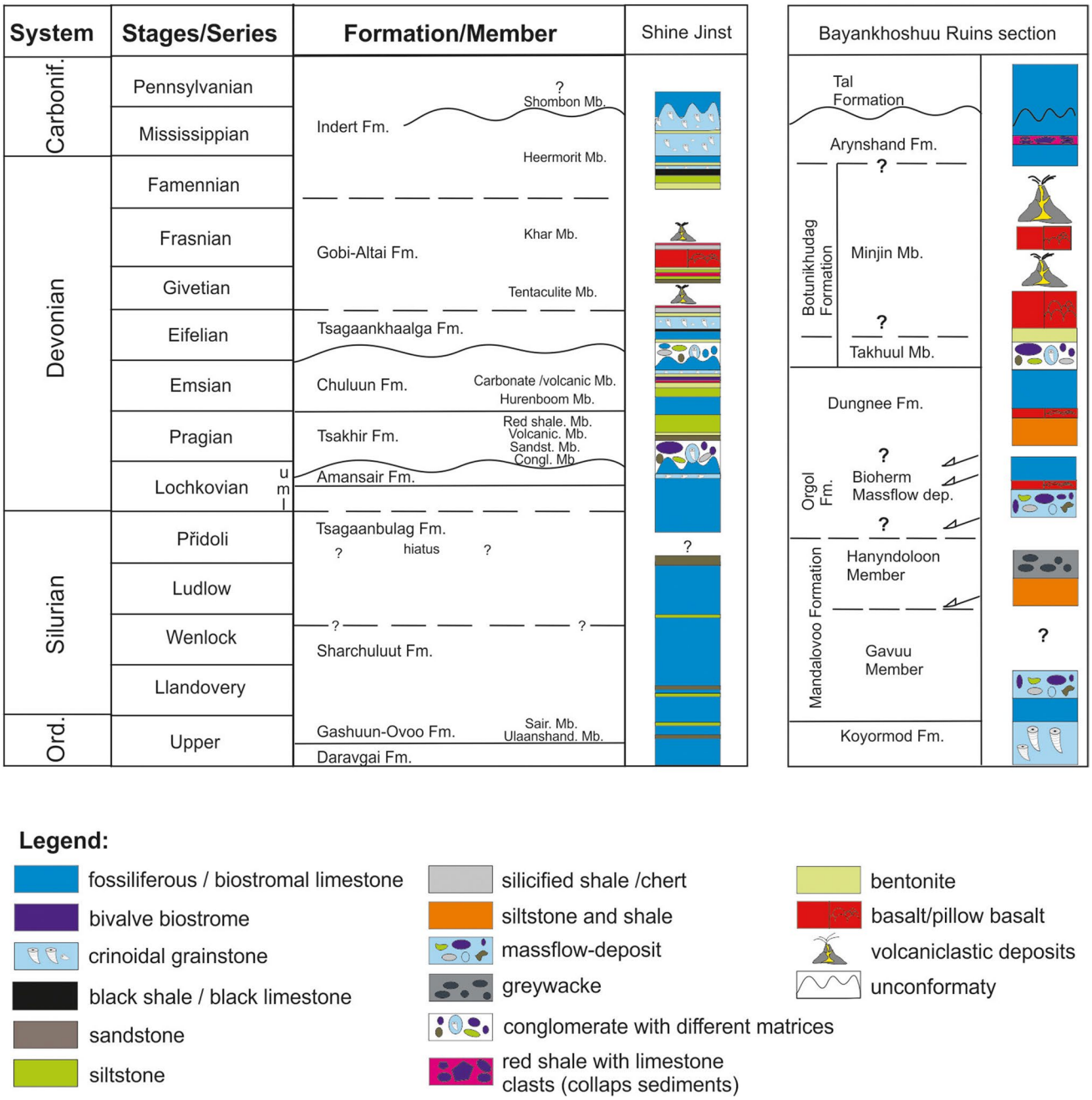


**Fig. 13:** Comparison of composite lithological logs from the Bayankhoshuu Ruins section (Mushgai region, southern Mongolia, see Munkhjargal et al. 2021) and the Shine Jinst region. Due to overall similar facies development it seems likely that the investigated regions belong to the same terrane

(carbonate ramp setting, see regional "encrinites" according to Aussich 1997) and dense crinoidal meadows may have occurred during different times (e.g. upper part of the Emsian Chuluun Formation, Eifelian Tsagaankhalga Formation, and particularly in the Late Devonian Indert Formation). It seems plausible that the occurrence of massive encrinites in the late Emsian (Chuluun Formation) demonstrates the recovery of the marine environment after the collapse of reefal ecosystems, similar to the recovery at the end of the Devonian (Sallan et al. 2011; Aussich and Kammer 2013).

Although Upper Devonian and lower Carboniferous rocks are known in several areas of Mongolia (Ariunchimeg et al. 2014, Suttner et al. 2020), the DCB is not documented in detail so far. It is clear that the remarkable facies difference of the Heermorit Member and the Shombon Member (Fig. 12c, d) does not represent the D/C boundary

as this boundary occurs within the Heermorit Member. *Protognathodus kockeli*, which was found in sample SHB-C-38 shows up just after the Hangenberg Event (Lane et al. 1980). This species is the name-giving species of the latest Famennian (Spalletta et al. 2017) and this revised conodont zone is equivalent to the Upper *praesulcata* and *sulcata* zones of Ziegler and Sandberg (1984). The definition of the base of the Carboniferous Period is defined by the first appearance datum (FAD) of *Siphonodella sulcata* in bed 69 of the valid GSSP at La Serre, southern France. Recent research and ongoing discussions (see Special Issue on that topic, Aretz and Corradini 2021 [Eds.]) have shown that alternative conodonts might be more useful, such as *Protognathodus kockeli*, which could define the D/C boundary (Corradini et al. 2011). In that sense, we can pinpoint the D/C boundary in the Shine Jinst region, but in our samples neither *Siphonodella praesulcata* or *Siphonodella sulcata* occur. The black shales below sample SHB-C-38 most probably are equivalents of the Hangenberg Black Shale and the D/C boundary should be between samples SBH-C-38 and sample SHB-C-40, which marks the *Siphonodella duplicata* Zone. The stratigraphic range of the Heermorit Member in our section is not known as conodont samples in the uppermost part did not yield conodonts. According to Minjin et al. (2001) the 360 m thick Shombon Member, which unconformably overlies the Heermorit Member yielded conodonts of the *Scaliognathus anchoralis –Doliognathus latus* Zone. Based on our results and data provided by Minjin et al. (2001) the Heermorit member of the Indert Formation most probably has a stratigraphical range from the *Bispathodus aculeatus aculeatus* Zone to the ? *Scaliognathus anchoralis –Doliognathus latus* Zone. Interestingly, the Arynshand Formation in southern Gobi Munkhjargal et al. (2021b) most likely ranges from the late *Bispathodus ultimus* conodont biozone to the *Scaliognathus anchoralis–Doliognathus latus* Zone and represents a ± similar stratigraphic range as the Heermorit Member of the Indert Formation. A tectonic breccia occurs in the early Mississippian in southern Gobi (Munkhjargal et al. 2021b), which is overlain by a red shale of remarkable thickness at the top of the Arynshand Formation Formation, which points to subaerial exposure in the early Mississippian (near the Tournaisian/Visean transition). It seems coeval with the erosional surface within the Indert Formation (transition of the Heermorit Member to the Shomboon Member) in our section. Although we have not recognised a hiatus between Devonian and Carboniferous rocks in the Shine Jinst section, Devonian rocks in Mongolia exhibit erosional surfaces in different stratigraphical levels and the stratigraphical record of Upper Devonian rocks and/or Mississippian rocks thus may differ from section to section in the investigated regions (see Fig. 2). In the CAOB Carmichael et al. (2016) have shown that directly below the D/C boundary an increased detrital supply occurs, which provides evidence for an eustatic drawdown in to an open-ocean island arc environment. These eustatic sea-level changes might be linked with local tectonics, such as amalgamation and uplift and later erosion of different terranes. Other Devonian/Carboniferous transitions in Mongolia exhibit hiatuses, e.g. as described from the Mandalovoo-Gurvansayhan terranes in southern Mongolia (Munkhjargal et al. 2021b).

Depositional similarities of the Mandalovoo-Gurvansayhan Terrane (Munkhjargal et al. 2021b) and the Gobi Altai Terrane (this report) are not restricted to the described conglomerates but occur in many parts of the succession ranging from the Ordovician to the early Carboniferous. For instance, both sections are dominated by limestones, intercalated are thick-bedded volcaniclastic rocks and basalts (e.g. Gobi Altai Formation, Fig. 13), shales (partly silicified such as in the Famennian) and siltstones, whereas pure sandstones are rare. Sedimentological differences are obvious during the Middle and Upper Devonian. Whereas Upper Devonian sediments in the Mushgai region (Mandalovoo-Gurvansayhan Terrane) are mainly composed of micritic fossiliferous limestones, which are slightly silicified in some horizons, more shallow-water, crinoidal limestones are the dominant sediment in the Shine Jinst region (e.g. crinoidal meadows). Intercalated are grey limestones and silicified, less fossiliferous limestones, and volcaniclastic rocks (see Fig. 8). Differences in the sedimentological record point to different facies settings along a passive margin and do not necessarily represent different structural units or even terranes. Thus, we assume that the Ordovician to Carboniferous successions of the study area and the sections described recently by Munkhjargal et al. (2021b) represent the same structural unit (passive margin), which belongs to the Mandalovoo Subzone proposed by Kröner et al. (2010). Instead of accretion of exotic terranes (Badarch et al. 2002), Kröner et al. (2010) concluded that the geology of SW Mongolia results from polyphase magmatic reworking of a Silurian-Devonian passive margin of a large microcontinent.

## Conclusions

An Early Devonian unconformity, which is linked with a regional tectonic event led to a profound change of reef communities in the late Early Devonian. Reef organisms such as corals and stromatoporoids occur but living conditions and/or geographic isolation resulted in less successful colonisation, so that reef organisms never accumulated enough to build real reefs. They grew as scattered colonies forming less densely populated biostromes. Diversity of reef builders is low. Endemic species of other fossil groups point to a rather geographically isolated position.

Unique large bivalves, which may belong to precursors of the Alatoconchidea family and remnants of an articulated Early Devonian fish belonging to chondrichthyan or acanthodian represent highlights of our expedition as those are extremely rare anywhere in the world.

Investigated sections are characterised by remarkable thick-bedded conglomerates in the Early and Middle Devonian, which point most probably to regional regressions. Volcanic activity increased during the Eifelian to Frasnian, which is documented by a large number of ash layers and basalts in the Tsagaankhaalga and Gobi-Altai formations. This part of the succession is similar to another section in southern Mongolia, which was considered to belong to another terrane in previous publications.

Thick-bedded crinoidal grainstones occur in different stratigraphical levels, suggesting a carbonate ramp setting, which was dominated by dense crinoidal meadows. The D/C boundary occurs most probably within the Heermorit Member of the Indert Formation. Based on new conodont results we recognised three Devonian events, which are described for the first time from Mongolia.

The overall facies development of the Shine Jinst region is very similar to coeval successions described by Munkhjargal et al. (2021b) for the Bayankhoshuu Ruins section in southern Mongolia. Occurring facies differences may be explained by lateral facies changes within a highly mobile depositional setting. Thus, it seems likely that both regions belong to the same tectonic unit, which is in accordance with data published by Macdonald et al. (2009) and Kröner et al. (2010).

**Supplementary Information** The online version contains supplementary material available at https://doi.org/10.1007/s12549-024-00608-3.

**Acknowledgements** We thank the entire Mongolian team for their tremendous support in preparing the expedition and facilitating our time in the field. Cara Cywinski assisted with field mapping. Magnus Karlsson provided real-time drone imagery for mapping. This paper is a contribution to IGCP`s 652 (Reading geologic time in Palaeozoic rocks: the need for an integrated stratigraphy) and 700 (Palaeozoic carbonate build-ups in Southeast Asia). The manuscript was significantly improved by the two reviewers Prof. Carlo Corradini and Prof. Clive Burrett. We thank Jana Anger for preparing conodont samples and polished slabs.

**Funding** Open Access funding enabled and organized by Projekt DEAL. P. Königshof received funding from Deutsche Forschungsgemeinschaft (DFG-KO-1622/19-2).

**Data availability** The material investigated in this study is stored in the following institutions: All fossils are stored at the Mongolian University of Science and Technology, Mongolia, whereas thin sections and polished slaps are stored at Senckenberg Research Institute and Natural History Museum Frankfurt, Germany (repository numbers see chapter "Material and methods").

## Declarations

**Conflict of Interest** The authors declare that they have no conflict of interest.



## References

Aboussalam, Z.S., Becker, R.T., & Bultynck, P. (2015). Emsian (Lower Devonian) conodont stratigraphy and correlation of the Anti Atlas (Southern Morocco). *Bulletin of Geosciences*, *90*(4), 893–980.

Alekseeva, R.E. (1993). Biostratigraphy of Devonian of Mongolia. *Joint Soviet-Mongolian Paleontological Expedition, 44*, 33–34. Moscow: Nauka Press. [in Russian]

Alekseeva, R.E., Aristov, V.A., Goryunova, R.V., Ulitina, L.M., & Erlanger, O.A. (1996). *Joint Soviet-Mongolian Paleontological Expedition*, *44*, 51–56. Moscow: Nauka Press. [in Russian]

Antoshkina, A., & Königshof, P. (2008). Lower Devonian reef structures in Russia: an example from the Urals. *Facies, 54*, 233–251.

Aretz, M., & Corradini, C. (2021). Global review of the Devonian-Carboniferous Boundary: An introduction. *Palaeobiodiversity and Palaeoenvironments*, *101*(2), 285–293. https://doi.org/10.1007/s12549-021-00499-8

Ariunchimeg, Y., Bayasgalan, A., Waters, J. A., Kido, E., Suttner, T. J., Sersmaa, G., Undariya, J., & Otgonbaatar, D. (2014). *IGCP 596 IGCP 580 Field Workshop Guidebook. 8-18th August, 2014, Ulaanbaatar, Mongolia* (pp. 1–55). Paleontological Center, Mongolian Academy of Sciences.

Aussich, W.I. (1997). Regional encrinites: A vanished lithofacies. In C. B. Brett, & G. C. Baird (Eds.), *Paleontological Events: Stratigraphic, Ecologic and Evolutionary Implications* (pp. 509–519). New York: Columbia University Press.

Aussich, W.I. (1999). Lower Mississippian Burlington Limestone along the Mississippi River Valley in Iowa, Illinois, and Missouri, USA, In W. I. Aussich, C. B. Brett, H. Hess, & M. J. Simms (Eds.), *Fossil Crinoids* (pp. 149–144). Cambridge: Cambridge University Press.

Aussich, W.I., & Kammer, T.W. (2013). Mississippian crinoid biodiversity, biogeography, and macroevolution. *Palaeontology*, *56*, 727–740.

Badarch, G., Cunningham, W.D., & Windley, B.F. (2002). A new terrane subdivision for Mongolia: Implications for the Phanerozoic crustal growth of Central Asia: *Journal of Asian Earth Sciences, 21*, 87–110, https://doi.org/10.1016/S1367-9120(02)00017-2

Bahrami, A., Gholamalian, H., Corradini, C., & Yazdi, M. (2011). Upper Devonian Conodont biostratigraphy of Shams Abad section, Kerman province, Iran. *Rivista Italiana di Paleontologica e stratigrafia*, *117*, 199–209.

Bardashev, I. (1990). Conodonts of Eifelian Stage of SSSR. (Konodonty eifel`skogo yarussa SSSR, red: V.G. Khalymbadzha *Izd. Kaz. Univerista*, 25–40. [in Russian]

Becker, R.T., Gradstein, F.M., & Hammer, O. (2012).The Devonian Period. In F. M. Gradstein, J. G. Ogg, M. D. Schmitz, & G. M. Ogg (Eds.), *A Geological Time Scale 2012*, Vol. 2 (pp. 559-601). Amsterdam: Elsevier.

Becker, R.T., Königshof, P., & Brett, C.E. (2016). Devonian climate, sea level and evolutionary events: an introduction. In R. T. Becker, P. Königshof, & C. E. Brett (Eds.), *Devonian Climate, Sea Level and Evolutionary Events. Geological Society, London, Special Publication*, *423*, 1–10.

Bischoff, G. (1957). Die Conodonten-Stratigraphie des rheno-herzynischen Unterkarbons mit Berücksichtigung der Wocklumeria-Stufe und der Devon/Karbon-Grenze. *Abhandlungen des hessischen Landesamtes für Bodenforschung*, *84*, 138–169.

Black, L.P., Kamo, S.L., Allen, C.M., Aleinikoff, J.N., Davis, D.W., Korsch, R.J., Foudoulis, C. (2003). TEMORA 1: a new zircon standard for Phanerozoic U–Pb geochronology. *Chemical Geology, 200(1–2), 155–170.*Blodgett, R.B., & Isozaki, Y. (2013). The Alatoconchidae, giant Permian Tethyan bivalve family, and the first occurrence in Alaska (McHugh Complex of the Chugach Terrane) and the Western Hemisphere. *Alaska Geology, 43*(8), 5–8.

Böhm, F., Dommergues, J.L., & Meister, C. (1995). Breccias of the Adnet Formation: Indicators of a Mid-Liassic tectonic event in the Northern Calcareous Alps (Salzburg/Austria). *Geologische Rundschau, 84*, 272–286.

Branson, E.B., & Mehl, M.G. (1934a). Conodonts from the Grassy Creek Shale of Missouri.*University of Missouri Studies*, *8*, 171–259.

Branson, E.B., & Mehl, M.G. (1934b). Conodonts from the Bushberg Sandstone and equivalent formations of Missouri. *University of Missouri Studies*, *8*, 265–299.

Brett, C.E., Baird, G.C., Bartholomew, A.J., DeSantis, M.K., & Ver Straeten C.A. (2011). Sequence stratigraphy and a revised sea-level curve for the Middle Devonian of eastern North America. *Palaeogeography, Palaeoclimatology, Palaeoecology, 304*, 21–53.

Bultynck, P. (1979). (with contributions by Hollard, H., García-Alcalde, J.L., House, M.R., & Soto, F.) Excursion in the Devonian of the Sierra de Guadarrama between Cercadillo and La Riba de Santiuste, 32–34. In J. L. García-Alcalde, et al. (Eds.), *Guidebook of the Field Trip, Meeting of the International Subcommission on Devonian Stratigraphy, Spain 1979*.

Bultynck, P. (1985). Lower Devonian (Emsian) – Middle Devonian (Eifelian and lowermost Givetian) conodont succession from the Ma`der and the Tafilalt, southern Morocco. *Courier Forschungsinstitut Senckenberg*, *75*, 262–286.

Bultynck, P. (1989). Conodonts from the La Grange Limestone (Emsian), Armorican Massif, North-Western France. *Courier Forschungsinstitut Senckenberg*, *117*, 173–203.

Carls, P., & Gandl, J. (1969). Stratigraphie und Conodonten des Unter-Devons der Östlichen Iberischen Ketten (NE-Spanien). *Neues Jahrbuch für Geologie und Paläontologie*, *Abhandlungen 132*, 155–218.

Carmichael, S.K., Waters, J.A., Batchelor, C.J., Coleman, D.M., Suttner, T.J., Kido, E., Moore, L.M., & Chadimová, L. (2016). Climate instability and tipping points in the Late Devonian: Detection of the Hangenberg Event in an open oceanic island arc in the Central Asian Orogenic Belt. *Gondwana Research, 32*, 213–231. https://doi.org/10.1016/j.gr.2015.02.009

Chatterton, B.D.E. (1974). Middle Devonian conodonts from the Harrogate Formation, southeastern British Columbia. *Canadian Journal of Earth Sciences*, *11*, 1461–1484.

Chen, J.F., Han, B.F., Ji, J.Q., Zhang, L., Xu, Z., He, G.Q., & Wang, T. (2010). Zircon U-Pb ages and tectonic implications of Paleozoic plutons in northern West Junggar, North Xinjiang, China. *Lithos, 115*, 137–152, https://doi.org/10.1016/j.lithos.2009.11.014

Chen, F., Xue, W., Yan, J., Wignall, P. B., Meng, Q., Luo, J., & Feng, Q. (2018). Alatoconchids: Giant Permian bivalves from South China. *Earth-Science Reviews, 179*, 147–167. https://doi.org/10.1016/j.earscirev.2018.01.012

Copper, P. (2002). Silurian and Devonian reefs: 80 Million years of global greenhouse between two ice ages. In W. Kiessling, E. Flügel, & J. Golonka (Eds.), *Phanerozoic Reef Patterns*. *Society for Sedimentary Geology (SEPM), Special publication, 72*, 181–238.

Copper, P., & Scotese, C.R. (2003). Megareefs in the Middle Devonian super greenhouse climates. *Special Publication of Geological Society of America, 370*, 209–230.

Corradini, C. & Corriga, M.G. (2012). A Přídoí-Lochkovian conodont zonation in Sardinia and the Carnic Alps: implications for a global zonation scheme. *Bulletin of Geosciences*, *87*(4), 635–650.

Corradini, C., Kaiser, S.I., Perri, M.C., & Spalletta, C. (2011). *Protognathodus* (Conodonta) and its potential as a tool for defining the Devonian/Carboniferous boundary. *Revista Italiana di Paleontologia e Stratigrafia*, *117*(1), 15–28.

Corriga, M.G., & Corradini, C. (2009). The conodont apparatus of *Zieglerodina eladioi* (Valenzuela Rios, 1994). *Bolletino della Società Paleontologica Italiana, 58,* 181–185.

Corriga, M.G., Corradini, C., Schönlaub, H-P., & Pondrelli, M. (2016). Lower Lochkovian (Lower Devonian) conodonts from Cellon section (Carnic Alps, Austria). *Bulletin of Geosciences*, *91*(2), 261–270.

Crônier, C., Ariuntogos, M., Königshof, P., Waters, J., & Carmichael, S.K. (2021). Late Devonian (Famennian) phacopid trilobites from western Mongolia. *Palaeobiodiversity and Palaeoenvironments*, *101*(3), 707–723. https://doi.org/10.1007/s12549-020-00449-w

Cunningham, W.D. (2010). Tectonic setting and structural evolution of the late Cenozoic Gobi Altai orogen. In T. M. Kusky, M.-G. Zhai, & W. Xiao (Eds.), The Evolving Continents: Understanding Processes of Continental Growth. *Geological Society of London Special Publication, 338*, 361–387, https://doi.org/10.1144/SP338.17

Debout, L., & Denayer, J (2018). Palaeoecology of the Upper Tournaisian (Mississippian) crinoidal limestones from South Belgium. *Geologica Belgica*, *21*/3-4, 111–127.

Donskaya, T.V., Gladkochub, D.P., & Mazukabzov, A.M. (2013). Late Paleozoic-Mesozoic subduction-related magmatism at the southern margin of the Siberian continent and the 150 million-year history of the Mongol-Okhotsk Ocean. *Journal of Asian Earth Sciences, 62,* 79–97. https://doi.org/10.1016/j.jseaes.2012.07.023

Fedo, C.M., Sircombe, K.N., & Rainbird, R.H. (2003). Detrital zircon analysis of the sedimentary record. *Reviews in Mineralogy and Geochemistry*, *53*, 277–303.

Frei, D., & Gerdes, A. (2009). Precise and accurate in situ U-Pb dating of zircon with high sample throughput by automated LA-SF-ICP-MS. *Chemical Geology*, *261*, 261–270.

Gerdes, A., & Zeh, A. (2006). Combined U-Pb and Hf isotope LA-(MC-)ICP-MS analyses of detrital zircons: Comparison with SHRIMP and new constraints for the provenance and age of an Armorican metasediment in Central Germany. *Earth and Planetary Science Letters*, *249*, 47–61.

Gibson, T.M. (2010). Sedimentology, depositional history and detrital zircon geochronology of the Lower Devonian Tsakhir Formation, Shine Jinst region, Mongolia. In A. P. de Wet, & L. Heister (Eds.), *Keck Geology Consortium Proceedings of the 23rd Annual Keck Research Symposium in Geology*, 194–20.

Gibson, T.M., Myrow, P.M., Macdonald, F.A., Minjin, C., & Gehreis, G.E. (2013). Depositional history, tectonics, and detrital zircon geochronology of Ordovician and Devonian strata in southwestern Mongolia. *Geological Society of America, Bulletin 2013, 125*(5-6), 877–893.

Hartenfels, S. (2011). Die globalen *Annulata*–Events und die Dasberg–Krise (Famennium, Oberdevon) in Europa und Nord-Afrika – hochauflösende Conodonten–Stratigraphie, Karbonat-,

Mikrofazies, Palökologie und Paläodiversität. *Münsterische Forschungen zur Geologie und Paläontologie*, *105*, 1–527.

Jackson, S.E., Pearson, N.J., Griffin, W.L., & Belousova, E.A. (2004). The application of laser ablation-inductively coupled plasma-mass spectrometry to in situ U-Pb zircon geochronology. *Chemical Geology*, *211*, 47–69.

James, N.P., & Bourque, P.A. (1992). Reefs and mounds. In R. G. Walker, & N. P. James (Eds.), *Facies Models: Response to Sea Level Change. Geological Association of Canada,* 323–347.

Johnson, J.G., Klapper, G., & Sandberg, C.A. (1985). Devonian eustatic fluctuations in Euramerica. *Geological Survey of America*, *Bulletin, 96*, 567–587.

Kaiser, S.I., Aretz, M., & Becker, R.T. (2016). The global Hangenberg Crisis (Devonian-Carboniferous transition): review of a first-order mass extinction. In R. T. Becker, P. Königshof, & C. E. Brett (Eds.), *Devonian climate, sea level and evolutionary events. Special Publications Geological Society of London 423*, 387–437. https://doi.org/10.1144/SP423.9

Kiessling, W., & Flügel, E. (2000). Late Paleozoic and Late Triassic limestones from North Palawan block (Philippines): microfacies and paleogeographical implications. *Facies, 43*(1), 39–77. https://doi.org/10.1007/BF02536984

Klapper, G. & Ziegler, W. (1967). Evolutionary developments of the *Icriodus latericrescens* group (Conodonts) in the Devonian of Europe and North America. *Palaeontographica, Abteilung A 23*, 199–224.

Klug, C.R. (1983). Conodonts and biostratigraphy of the Muscatatuck Group (Middle Devonian), south-central Indiana and north-central Kentucky.*Wisconsin Academy of Sciences, Arts and Letters*, *71*(1), 79–112.

Königshof, P., & Flick, H. (in press). Fringing reef growth in the mid-Devonian: An example from the southern Rhenish Massif, Germany. In S. Hartenfels, C. Hartkopf-Froeder, & P. Königshof (Eds.), *The Rhenish Massif: More than 150 years of research in a Variscan mountain chain, part II. Palaeobiodiversity and Palaeoenvironments*. https://doi.org/10.1007/s12549-023-00591-1. [published online in 2023]

Königshof, P., Loos, S. & Rutkowski, J. (in press a). Lithofacies variability and facies analysis of a Givetian reef Complex in the southwestern Lahn Syncline (Rhenish Massif, Germany). In S. Hartenfels, C. Hartkopf-Froeder, & P. Königshof (Eds.), *The Rhenish Massif: More than 150 years of research in a Variscan mountain chain, part II. Palaeobiodiversity and Palaeoenvironments*. https://doi.org/10.1007/s12549-023-00585-z. . [published online in 2023]

Königshof, P., Jansen, U., Linnemann, U., & Mende, K. (in press b). The Rhenish Massif. In U. Linnemann (Ed.), *The Geology of the Variscan orogen in Central and Eastern Europe – From the margin of Gondwana to the center of Pangea.* Cham: Springer.

Kröner, A., Lehmann, J., Schulmann, K., Demoux, A., Lexa, O., Tomurhuu, D., Stipská, P., Liu, D.Y., & Wingate, M.T.D. (2010). Lithostratigraphic and geochronological constraints on the evolution of the Central Asian Orogenic Belt in SW Mongolia: Early Paleozoic rifting followed by Late Paleozoic accretion. *American Journal of Science, 310*, 523–574, https://doi.org/10.2475/07.2010.01

Kröner, A., Kovach, V., Belousova, E., Hegner, E., Armstrong, R., Dolgopolova, A., Seltmann, R., Alexeiev, D.V., Hoffmann, J.E., Wong, J., Sun, M., Cai, K., Wang, T., Tong, Y., & Wilde, S.A. (2014). Reassessment of continental growth during the accretionary history of the Central Asian Orogenic Belt. *Gondwana Research, 25,* 103–125.

Lamb, M.A., & Badarch, G. (1997). Paleozoic sedimentary basins and volcanic arc systems of Southern Mongolia: New stratigraphic and sedimentological constrains. *International Geology Review, 39*, 542–576.

Lamb, M.A., & Badarch, G. (2001). Paleozoic sedimentary basins and volcanic arc systems of southern Mongolia: new geochemical and petrographic constraints. In M.S. Hendrix, & G.A. David (Eds.), Paleozoic and tectonic evolution of central Asia: From continental assembly to intracontinental deformation. Boulder, Colorado. *Geological Society of America Memoir, 194*, 117–149.

Lamb, M.A., Badarch, G., Navratil, T., & Poier, R. (2008). Structural and geochronologic data from the Shine Jinst area, eastern Gobi Altai, Mongolia: Implications for Phanerozoic intracontinental deformation in Asia. *Tectonophysics, 451*, 312–330, https://doi.org/10.1016/j.tecto.2007.11.061

Lane, H.R., Sandberg, C.A., & Ziegler, W. (1980). Taxonomy and phylogeny of some Lower Carboniferous conodonts and preliminary standard post-Siphonodella zonation. *Geologica et Palaeontologica*, *14*, 117– 164.

Lehmann, J., Schulmann, K. Lexa, O., Corsini, M., Kröner, A., Stipská, P., Tomurhuu, D., & Otgonbator, D. (2010). Structural constraints on the evolution of the Central Asian Orogenic Belt in SW Mongolia. *American Journal of Science, 310*, 575–628, https://doi.org/10.2475/07.2010.02

Link, P.K., Fanning, C.M., Beranek, L.P. (2005). Reliability and longitudinal change of detrital-zircon age spectra in the Snake River system, Idaho and Wyoming: An example of reproducing the bumpy barcode. *Sedimentary Geology*, *182*, 101–142.

Ludwig, K.R. (2008). Users manual for Isoplot 3.70 - A geochronological toolkit for Microsoft Excel. *Berkeley Geochronology Center Special Publication*, *No.4*, 1–76.

Macdonald, F.A., Jones, D.S., & Schrag, D.P. (2009). Stratigraphic and tectonic implications of a new glacial diamictite-cap carbonate couplet in southwestern Mongolia: *Geology, 37*, 123–126, 10.1130 /G24797A.1.

MacNeil, A.J., & Jones, B. (2016). Stromatoporoid growth forms and Devonian reef fabrics in the Upper Devonian Alexandra Reef System, Canada – Insight on challenges of applying Devonian reef facies models. *Sedimentology, 63*, 1425–1457.

May, A., & Rodríguez, S. (2012). Pragian (Lower Devonian) stromatoporoids and rugose corals from Zújar (Sierra Morena, southern Spain). *Geologica Belgica*, *15*(4), 226–235.

Minjin, Ch., Sersmaa, G., Ariunchimeg, Ya., Gereltsetseg, L., Undarya, J., Tumenbayar, B., & Bolortsetseg, M. (2001). *The guide book, Abstract and Ordovician – Silurian correlation chart for the joint field meeting of IGCP 410 and IGCP 421 in Mongolia. Part II. Mongolian Field Guide*, 12–90.

Munkhjargal, A., Königshof, P., Hartenfels, S., Jansen, U., Nazik, A., Carmichael, S.K., Waters, J.A., Gonchigdorj, S., Crônier, C., Ariunchimeg, Ya, Paschall, O., & Dombrowski, A. (2021a). The Hushoot Shiveetiin gol section (Baruunhuurai Terrane): Sedimentology and facies from a Late Devonian island arc setting. *Palaeobiodiversity and Palaeoenvironments*, *101*(3), 663–687. https://doi.org/10.1007/s12549-020-00445-0

Munkhjargal, A., Königshof, P., Waters, J.A., Carmichael, S.K., Gonchigdorj, S., Thassanapak, H., Udchachon, M., & Sharav, D. (2021b). The Mandalovoo–Gurvansayhan terranes in the Southern Gobi of Mongolia: new insights from the Bayankhoshuu Ruins section. *Palaeobiodiversity and Palaeoenvironments, 101*(3), 755–780. https://doi.org/10.1007/s12549-020-00471-y

Murphy, M.A., & Valenzuela Rios, J.I. (1999). *Lanea* new genus, lineage of Early Devonian conodonts. *Bollettino-Società Paleontologica Italiana*, *37*(2), 321 –334.

Nazik, A., Königshof, P., Ariuntogos, A., Waters, J.A., & Carmichael, S.K. (2021). Late Devonian ostracods from the Late Devonian Hushoot Shiveetiin gol section (Baruunhuurai Terrane, western Mongolia) and their palaeoenvironmental implication and palaeobiogeographic relationship. *Palaeobiodiversity and*

*Palaeoenvironments, 101*(3), 689–706. https://doi.org/10.1007/s12549-020-00446-z

Nyamsuren, G. (1999). New data on Devonian and Carboniferous biostratigraphy in southern Mongolia. *Transactions, Institute of Geology and Mineral Resources, 13*, 70–74.

Over, D.J., Sullivan, NB., Peteya, J., Minjin, C., Myrow, P.M., & Soja, C.M. (2011). Conodonts from the Tsagaanhaalga Formation (Emsian? – Eifelian) and the Tentaculite Member of the Govialtai Formation (Eifelian – Givetian), Tsakir Well Section, Govi Altai Terrane, Southern Mongolia. *Geological Society of America, Abstract with Programs*, *43*(1), p. 75.

Pellegrini, A.F.A., Soja, C.M., & Minjin C. (2012). Post-tectonic limitations on Early Devonian (Emsian) reef development in the Gobi-Altai Region, Mongolia. *Lethaia, 45*, 46–61.

Philip, G.M. (1965).Lower Devonian conodonts from the Tyers Area, Gippsland, Victoria. *Proceedings of the Royal Society of Victoria*, *79*(1), 95–115.

Pohler, S.M-L. (1998). Devonian Carbonate Buildup Facies in an Intra-oceanic Island Arc (Tamworth belt, New South-Wales, Australia). *Facies*, *39*, 1–34.

Puetz, S.J. (2018). A relational database of global U-Pb ages. *Geoscience Frontiers*, *9*, 877–891.

Reitman, N.G. (2010). Palaeoecology and chemostratigraphy of the Amansair and Tsagaanbulag formations, Gobi-Altai Terrane, Mongolia. *23rd Annual Keck Symposium*: 2010, Houston, Texas, (extended abstracts), 229–237.

Roelofs, B., Königshof, P., Trinajstic, K., & Munkhjargal, A. (2021). Vertebrate microremains from the Late Devonian (Famennian) of western Mongolia. *Palaeobiodiversity and Palaeoenvironments, 101*(3), 741–753. https://doi.org/10.1007/s12549-021-00503-1

Rozman, K.S., & Minjin, Ch. (1988). Silurian stratigraphy of the Gobi Altai, southern Mongolia. *Doklady Akademii Nauk SSSR*, *301*, 932–935.

Ruzhentsev, S.V., & Pospelov, I.I. (1992). The South Mongolia Variscian fold system. *Geotectonics, 30*, 383–395.

Sallan, L.C., Kammer, T.W., Aussich, W.I., & Cook, L.A. (2011). Persistent predator-prey dynamics revealed by mass extinctions. *Proceedings of the National Academy of Sciences*, *108*/20, 8335–8338. https://doi.org/10.1073/pnas.1100631108

Şengör, A.M.C., Natal'in, B.A., & Burtman, V.S. (1993). Evolution of the Altaid tectonic collage and Paleozoic crustal growth in Eurasia. *Nature*, *364*, 299–307. https://doi.org/10.1038/364299a0

Shen, J.-W., Webb, G.E., & Jell, J.S. (2008). Platform margins, reef facies, and microbial carbonates; a comparison of Devonian reef complexes in the Canning Basin, Western Australia, and the Guilin region, South China. *Earth-Science Reviews, 88*, 33–59.

Sláma, J., Košler, J., Condon, D.J., Crowley, J.L., Gerdes, A., Hanchar, J.M., Horstwood, M.S.A., Morris, G.A., Nasdala, L., Norberg, N., Schaltegger, U., Schoene, B., Tubrett, M.N., & Whitehouse, M.J. (2008). Plešovice zircon — A new natural reference material for U-Pb and Hf isotopic microanalysis. *Chemical Geology*, *249*, 1–35.

Soja, C.M., Minjin, C., Myrow, P., & Over, D.J. (2010). Paleozoic paleoenvironmental reconstruction of the Gobi-Altai terrane, Mongolia. In A. P. de Wet, & L. Heister (Eds.), *Keck Geology Consortium Proceedings of the 23rd Annual Keck Research Symposium in Geology*, 182–199.

Spalletta, C., Perri, M.C., Over, D.J., & Corradini, C. (2017). Famennian (Upper Devonian) conodont zonation: revised global standard. *Bulletin of Geosciences*, *92*(1), 31–57.

Stacey, J.S., & Kramers, J.D. (1975). Approximation of terrestrial lead isotope evolution by a two-stage model. *Earth and Planetary Science Letters*, *26*, 207–221.

Stearn, C.W. (2001). Biostratigraphy of Devonian stromatoporoid faunas of Arctic and Western Canada. *Journal Paleontology*, *23*, 229–232. https://doi.org/10.1666/0022-3360(2001)075<0009:BODSFO>2.0.CO;2

Stewart, G.R. & Sweet, W.C. (1956). Conodonts from the Middle Devonian bone bed of central and West-central Ohio. *Journal of Paleontology*, *30*(2), 261–273.

Sullivan, N.B., Over, J.D., Chuluun, M., & Myrow, P.M. (2016). Subsidence and drowning of a carbonate platform in south-central Mongolia (Gobi Altai region) during late Eifelian to early Givetian: A synthesis of conodont data, magnetic susceptibility, and palaeoecology. *Journal of Asian Earth Sciences*, *115*, 204–213.

Suttner, T.J., Kido, E., Ariunchimeg, Y., Sersmaa, G., Waters, J.A., Carmichael, S. K., Batchelor, C.J., Ariuntogos, M., Hušková, A., Slavík, L., Valenzuela-Ríos, J.I., Liao, J.-C., & Gatovsky, Y. A. (2020). Conodonts from Late Devonian island arc settings (Baruunhuurai Terrane, western Mongolia). *Palaeogeography, Palaeoclimatology, Palaeoecology, 549*, 1–122. https://doi.org/10.1016/j.palaeo.2019.03.001

Ta, H.-P., Königshof, P., Ellwood, B.-B., Nguyen, T.C., Luu, P.L.T., Doan, D.H., & Munkhjargal, A. (2022). Facies, magnetic susceptibility and timing of the Late Devonian Frasnian/Famennian boundary interval (Xom Nha Formation, Central Vietnam). *Palaeobiodiversity and Palaeoenvironments, 102*(1), 129–146.

Talent, J.A. & Yolkin, E.A. (1987). Transgression-Regression Patterns for the Devonian of Australia and Southern West Siberia. *Courier Forschungsinstitut Senckenberg*, *92*, 235–249.

Tomurtogoo, O. (1997). A new tectonic scheme of the Paleozoides in Mongolia. *Mongolian Geoscientist, 3*, 12–17.

Udchachon, M., Burrett, C., Thassanapak, H., Chonglakmani, C., Campbell, H., & Feng, Q. (2014). Depositional setting and paleoenvironment of an alatoconchid-bearing Middle Permian carbonate ramp sequence in the Indochina Terrane. *Journal of Asian Earth Sciences, 87*, 37–55. https://doi.org/10.1016/j.jseaes.2014.02.012

Ulitina L.M., Bol'shakova L.N., & Kopajevich G.V. (1976). Particular occurrence of the Stromatoporoidea, Rugosa and Bryozoa within Paleozoic sequence of Dzhinsetu-Ula Mountains (Gobian Altai). In Paleontology and Biostratigraphy of Mongolia; *Joint Soviet-Mongolian Paleontological Expedition*, *3*, 327–340 Moscow: Nauka Press, Trans. [in Russian]

Underwood, J.N., Smith, L.D., Oppen, M.J.H. van, & Gilmour, J.P. (2009). Ecologically relevant dispersal of corals on isolated reefs: implications for managing resilience. *Ecological Applications, 19*, 18–29.

Uyeno, T.T. (1991). Pre-Famennian Devonian conodont biostratigraphy of selected intervals in the eastern Canadian Cordillera. In M. J. Orchard, & A. D. McCracken (Eds.), Ordovician to Triassic conodont Paleontology of the Canadian Cordillera. *Geological Survey of Canada*, *Bulletin, 417*, 129–161.

Uyeno, T.T. & Lesperance, P.J. (1997). Middle Devonian (Eifelian) conodonts and their stratigraphic implications from the mid-Appalachians of Quebec. *Geological Survey of America*, *Special Paper*, *321*, 145–160.

Voges, A. (1959). Conodonten aus dem Unterkarbon I und II (Gattendorfia- und Pericyclus-Stufe) des Sauerlandes. *Paläontologische Zeitschrift*, *33*, 266–314.

Wang, C.Y., Ziegler, W., Minjin, Ch., Munchsetseg, J., Gerelsetseg, J., & Undarya, J. (2003). The first discovery of middle Lochkovian (Devonian) conodonts from the South Gobi, Mongolia. *Science in China (D Series)*, *33*(10), 975–980.

Wang, C.Y., Weddige, K., & Minjin, Ch. (2005a). Age revision of some Palaeozoic strata of Mongolia based on conodonts. *Journal of Asian Earth Sciences, 25*, 759–771.

Wang, C.Y., Chuluun, M., Weddige, K., Ziegler, W., Gonchigdorj, S., Jugdernamjil, M., Lhagva, G., & Jalbaa, U. (2005b). Devonian (Emsian – Eifelian) Conodonts from South Gobi, Mongolia. *Acta Micropalaentologica Sinica, 22*(1), 19–28.

Waters, J.A., & Sevastopulo, G.D. (1984). The stratigraphical distribution and palaeoecology of Irish Lower Carboniferous blastoids. *Irish Journal of Earth Sciences*, *6*, 137–154.

Waters, J.A., Waters, J.W., Königshof, P., Carmichael, S.K., & Ariuntogos, M. (2021). Famennian crinoids and blastoids (Echinodermata) from Mongolia. *Palaeobiodiversity and Palaeoenvironments*, *101*(3), 725–740. https://doi.org/10.1007/s12549-020-00450-3

Waters, J.A., Waters, J.W., Carmichael, S.K., Königshof, P., Munkhjargal, A., & Gonchigdorj, S. (2023). The Central Asian Orogenic Belt (Western China and Mongolia) was a biodiversity hotspot in the Late Devonian. *Geological Society of America, Abstracts with Programs, 2023.*

Webster, G.D. (2003). Bibliography and index of Paleozoic crinoids, coronates, and hemistreptocrinoids. *Geological Society of America*, *Special Paper*, *362*, 1758–1999.

Weddige, K. (1977). Die Conodonten der Eifel-Stufe im Typusgebiet und in benachbarten Faziesgebieten. *Seckenbergiana lethaea*, *65*, 179–223.

Wilson, J. L. (1975). *Carbonate facies in geologic history* (pp. 1–471). New York: Springer.

Windley, B.F., Alexeiev, D., Xiao, W., Kröner, A., & Badarch, G. (2007). Tectonic models for accretion of the Central Asian Orogenic Belt. *Journal of the Geological Society, 164,* 31–47. https://doi.org/10.1144/0016-76492006-02

Wittekindt, H. (1966). Zur Conodontenchronologie des Mitteldevons. *Fortschritte in der Geologie von Rheinland und Westfalen*, *9*, 621–646.

Xiao, W., & Santosh, M. (2014). The western Central Asian Orogenic Belt: A window to accretionary orogenesis and continental growth. *Gondwana Research, 25*(4), 1429–1444. https://doi.org/10.1016/j.gr.2014.01.008

Xiao, W., Han, C., Yuan, C., Sun, M., Lin, S., Chen, H., Li, Z., Li, J., & Sun, S. (2008). Middle Cambrian to Permian subduction-related accretionary orogenesis of Northern Xinjiang, NW China: Implications for the tectonic evolution of central Asia: *Journal of Asian Earth Sciences, 32*, 102–117, https://doi.org/10.1016/j.jseaes.2007.10.008

Xiao, W. J., Huang, B. C., Han, C. M., Sun, S., & Li, J. L. (2010). A review of the western part of the Altaids: A key to understanding the architecture of accretionary orogens. *Gondwana Research, 18*(2–3), 253–273. https://doi.org/10.1016/j.gr.2010.01.007

Yancey, T.E., & Boyd, D. (1983).Revision of the Alatoconchidae – a remarkable family of Permian bivalves. *Palaeontology, 26*, 497–520.

Yang, G., Li, Y., Tong, L., & Yang, B. (2015). Oceanic Island Basalts from the Darbut and Karamay Ophiolitic Mélange in West Junggar (NW China): Product of a Middle Devonian Mantle Plume? *Acta Geologica Sinica, 89,* 105–106. https://doi.org/10.1111/1755-6724.12308_63

Yang, G., Li, Y., Tong, L., Wang, Z., Duan, F., Xu, Q., & Li, H. (2019). An overview of oceanic island basalts in accretionary complexes and seamounts accretion in the western Central Asian Orogenic Belt. *Journal of Asian Earth Sciences, 179*, 385–398. https://doi.org/10.1016/j.jseaes.2019.04.011

Ziegler, W. (1956). Unterdevonische Conodonten, insbesondere aus dem Schönauer und dem *Zorgensis*-Kalk. *Notitzblätter des hessischen Landesamtes für Bodenforschung*, *84*, 93–106.

Ziegler, W. (1962). Taxionomie und Phylogenie Oberdevonischer Conodonten und ihre stratigraphische Bedeutung. *Abhandlungen des hessischen Landesamtes für Bodenforschung*, *38*, 1–166.

Ziegler, W. (1969). Eine neue Conodontenfauna aus dem höchsten Oberdevon. *Fortschritte Geologie von Rheinland und Westfalen*, *17*, 179–191.

Ziegler, W., & Sandberg, C.A. (1984). Palmatolepis-based revision of upper part of standard Late Devonian conodont zonation. *Geological Society of America Special Paper*, *196*, 179–194.

Ziegler W. & Sandberg C.A. (1990).The Late Devonian Standard Conodont Zonation. *Courier Forschungsinstitut Senckenberg*, *121*, 1–115.

## Authors and Affiliations

**Peter Königshof[1] · Sarah K. Carmichael[2] · Johnny A. Waters[2] · Will Waters[3] · Ariuntogos Munkhjargal[1,4] · Sersmaa Gonchigdorj[4] · Catherine Crônier[5] · Atike Nazik[6] · Katie Duckett[2,7] · Jenny Foronda[2] · Johannes Zieger[8] · Ulf Linnemann[8]**

✉ Peter Königshof
peter.koenigshof@senckenberg.de

Sarah K. Carmichael
carmichaelsk@appstate.edu

Johnny A. Waters
watersja@appstate.edu

Will Waters
willwaters_1@hotmail.com

Ariuntogos Munkhjargal
ariuka.munkhjargal@senckenberg.de

Sersmaa Gonchigdorj
sersmaa@gmail.com

Catherine Crônier
catherine.cronier@univ-lille.fr

Atike Nazik
anazik@cu.edu.tr

Katie Duckett
katieduckett4@gmail.com

Jenny Foronda
forondajr@appstate.edu

Johannes Zieger
johannes.zieger@senckenberg.de

Ulf Linnemann
ulf.linnemann@senckenberg.de

1 Senckenberg Research Institute and Natural History Museum Frankfurt, Senckenberganlage 25, 60325 Frankfurt am Main, Germany

2 Department of Geological and Environmental Sciences, Appalachian State University, 572 Rivers St., Boone, NC 28608, USA

3 Houston, Texas, USA

4 Mongolian University of Science and Technology 8th khoroo, Baga Toiruu 34, Sukhbaatar District, 14191 Ulaanbaatar, Mongolia

5 Université de Lille, CNRS, UMR 8198 Évo-Éco-Paléo, 59000 Lille, France

6 Faculty of Engeneering Department, Cukurova University, Mithat Özsan Bulvari, 01330 Adana, Turkey

7 R.O.O.T., LLC, Glenwood Springs, CO 81601, USA

8 Senckenberg Naturhistorische Sammlungen Dresden, GeoPlasmaLab, Königsbrücker Landstrasse 159, 01109 Dresden, Germany